Accepted Manuscript

Exergy assessment and exergy cost analysis of a renewable-based and hybrid trigeneration scheme for domestic water and energy supply

Sergio Usón, Javier Uche, Amaya Martínez, Alejandro del Amo, Luis Acevedo, Ángel Bayod

PII: S0360-5442(18)32335-1

DOI: https://doi.org/10.1016/j.energy.2018.11.124

Reference: EGY 14222

To appear in: *Energy*

Received Date: 30 March 2018

Revised Date: 16 September 2018

Accepted Date: 26 November 2018

Please cite this article as: Usón S, Uche J, Martínez A, del Amo A, Acevedo L, Bayod Á, Exergy assessment and exergy cost analysis of a renewable-based and hybrid trigeneration scheme for domestic water and energy supply, *Energy* (2018), doi: https://doi.org/10.1016/j.energy.2018.11.124.

Exergy assessment and exergy cost analysis of a renewable-based and hybrid trigeneration scheme for domestic water and energy supply

Sergio Usón*[1], Javier Uche[1], Amaya Martínez[1], Alejandro del Amo[2], Luis Acevedo[3], Ángel Bayod[1]

[1] Universidad de Zaragoza, CIRCE Institute.

[2] Abora Solar SL.

[3] CIRCE Foundation, Process Integration Group.

*Corresponding author e-mail: suson@unizar.es

Abstract

Exergy and exergy cost analyses are proposed as complementary methods for the assessment and better understanding of the efficiency of a hybrid trigeneration system based on renewable energy sources. The system combines photovoltaic/thermal collectors, an evacuated tube collector and a wind turbine and produces electricity, sanitary hot water and desalted fresh water for a single family house. The system includes two desalination technologies (reverse osmosis and membrane distillation) that consume power and heat respectively, and two kinds of energy storage devices (a hot water tank and two lead-acid batteries).

The assessment is based on simulations developed by using TRNSYS software. As a first level of detail, exergy analysis is applied in ten-minute basis to selected plant components. As a second level of detail, it is proposed to apply exergy-based indicators that summarize the system behavior during a longer period of time (monthly basis). By using aggregated values, exergy accumulation terms become negligible, what allows applying symbolic thermoeconomics to calculate exergy cost

and to analyze in depth the process of cost formation. The system has an exergy efficiency of 7.76% (6.68 due to electricity, 0.33 due to fresh water and 0.75 due to sanitary hot water).

Keywords: Renewable energy, hybrid systems, polygeneration, desalination, photovoltaic-thermal collector.

1. Introduction

The use of solar energy can constitute a sustainable option for providing electricity, thermal and cooling energy or even fresh water (FW) [1]. In particular, photovoltaic-thermal (PVT) collectors integrate the production of both electricity and hot water, improving the overall efficiency and reducing the required roof surface [2-4]. Since not always it is possible to have abundant wind or solar irradiance, wind-solar hybrid systems are usually proposed for isolated systems [5-6]. Regarding water production, membrane distillation (MD) operates at temperatures about 70-90 ºC [7], so that it is suitable for being integrated with different kinds of solar thermal collectors like the evacuated tube (ETC) that can also activate an absorption chiller [8]. At a wider scale, concentrated solar power (CSP) technologies could be linked to large-scale desalination units to provide affordable costs for fresh water [9]. Alternatively, solar photovoltaics (PV) can supply some power to feed a Reverse Osmosis unit (RO) [10] or integrated in a solar still to produce some amount of distillate [11].

The term polygeneration is commonly understood as the combined generation of several products provided by the supply of one or several fuels, which can be renewable sources. The use of fossil fuels is usually linked to huge installations [12] and several integrations have been studied in depth [13], or the same technology has

been tested in different arrangements [14-15]. The use of Renewable Energy Sources (RES) and in particular solar energy has been also extensively analyzed. PVT have been linked to power, heating and cooling [16] and sometimes fresh water provided by desalination is one of the products in those RES-based integrated schemes, especially in dry and isolated areas. PVT can be linked to absorption chillers and multi-effect distillation (MED) [17], but this combined production can be also obtained by biomass feeding an Organic Rankine Cycle (ORC) [18]. Sometimes PVT is substituted by hybrid RES like solar and biomass [19] or some fraction of fossil fuels and RES [20]. Unfortunately, all those references were restricted to numerical analyses and were not validated with experimental tests. Thus, very few examples can be found in the validation of integrated PVT schemes and without desalination [21], being solar thermal one validated integration with MD distillate and chilled water [22-23].

Besides, exergy analysis [24] is able to detect and quantify in detail where and when irreversibility occurs and, thus, it is useful in the search for new improvements of energy intensive systems. Furthermore, it quantifies in the same units streams of different nature, what makes it very convenient for the assessment of polygeneration systems. From independent to integrated systems, exergy analysis of PV and then PVT has been developed by Saloux et al. [25]. Hybrid desalination (MED+RO) has also been analyzed from the point of view of irreversibility minimization [26]. Very low exergy efficiency of a MD supplied by a solar thermal collector was yet observed [27]. Thermodynamic efficiency of the combined production of desalted water and power has been also analyzed in depth. If solar energy combines power generation, exergoeconomic analysis can provide costs for water and power by using CSP+MED [28] or two solar schemes (one helped by an ORC) + MED [29]. The same can be

found in case of using fossil fuels even by desalting by hybrid techniques [12,30]. In polygeneration schemes, exergy analysis provides useful information about the rational path in the efficiency of conversion processes involved. Several examples can be found in literature, from a typical scheme based on an internal combustion engine (ICE), absorption chiller (LiBr-H_2O) and heat exchanger (HX) in order to find out the best operation strategy [31], up to a more complex scheme based on a solid oxide fuel cell (SOFC), GAX cooling cycle and HX [32], or that one using refuse derived fuel (RDF) to produce additional syngas and H_2 apart from power, heat and cold to a District Heating and Cooling (DHC) network [33]. If exergy analysis is extended to the use of RES in integrated polygeneration schemes, usually hybrid sources are taken, being solar-geothermal one option to provide power, heating and SHW [34] or cooling and industrial heating [35], or the binomial solar-biomass for the same trigeneration purposes with heat used for heating [36] or heated air [37]. Few examples of full integration of RES based polygeneration systems including desalination can be found in the literature. In [38], Calise and coworkers developed an exergy and exergoeconomic analysis of a polygeneration system based on parabolic collectors, biomass boiler, absorption chiller and MED; in [39], geothermal energy and an ORC complemented the solar field to improve the overall efficiency of the already proposed polygeneration system. Low temperature geothermal sources have been also studied to produce fresh water (FW), hot water and electricity by means of a heat transformer (HT), an ORC and a single-stage evaporation desalination process [40]. Nevertheless, hybrid desalination has not been considered yet in those multipurpose analyses.

Thermoeconomic analysis [41,42] goes a step further of exergy analysis by introducing the concept of exergy cost, which is the amount of exergy resources

consumed by a given system for producing an exergy stream within that system. Unit exergy cost is calculated by dividing exergy cost into the exergy of the stream considered. Symbolic thermoeconomic provides a matrix-based methodology for exergy cost calculation that is able to analyze the process of cost formation, as a result of the effects of irreversibility taking place in the different components of the system [43-44]. Finally, in [45] a methodology for cost decomposition according to resources consumed by the system is proposed, which is useful when a multi-resource facility is analyzed. In this sense, cost allocation is a recurrent issue in multipurpose schemes [46] including the hybrid supply [47]. For the case of desalination, energy cost allocation of water [48] and the use of exergy costing has been even applied [49], sometimes diagnosis of inefficiencies was also assessed [50]. Again, the exergy cost analysis for a multipurpose scheme based on RES that includes desalination is rather difficult to find, one example could be the work of Leiva et al. [51] but oriented to huge desalination facilities (MED) based on CSP technologies, or the abovementioned studies [38-40]. Besides, the cost calculation was based on exergy cost balances and results were given in economic terms, but a detailed cost formation analysis were not included and steady state models were applied.

In this paper, the exergy and exergy cost analyses of the transient operation of a domestic, hybrid and renewable energy-based polygeneration system that includes PVT, evacuated tubes collector (ETC), a wind turbine and two water production technologies (reverse osmosis, RO and membrane distillation, MD) is developed. This integrated scheme is the result of an in-depth design analysis of available commercial domestic RES-based technologies that can cover the demands of power, SHW and FW for a typical dwelling isolated from the grids [52]. Hybrid RES provide

power and heat that can flexibly dedicated to cover power demands or feed the RO unit, and heat that can be consumed in providing SHW or producing distillate fresh water in the MD. Furthermore, RES variability is smoothed by the energy storage in batteries and hot water tank. Data for exergy calculations have been obtained from TRNSYS simulations along a complete year; although an experimental facility has been built based on the design presented in the paper, data from this pilot plant has been obtained only for selected days and not covering the whole year, which is required for the analysis. Besides detailed analysis (ten-minute basis), aggregated exergy-related parameters are calculated (monthly basis and yearly basis). This allows to calculate unit exergy costs and to analyze the formation process of these costs, with the final aim of knowing the overall thermodynamic performance of the installation in its life cycle. With this information, guidelines for the best operation of those integrated schemes, or the priority in the use of available resources to cover a specific demand of the dwelling (power, SHW or FW), could be afforded from the point of view of the thermodynamic efficiency. As far as the authors' knowledge, this is the first analysis combining exergy, exergy cost, and exergy cost formation for an integrated scheme producing heat and power by two RES, which can be consumed by different devices including two different desalination technologies.

2. Methodology

The aim of this section is to present the framework needed for obtaining the exergy-related parameters which constitute the results of the paper. First, the polygeneration system is presented. Then, a brief outline of the TRNSYS model is made. Afterwards, equations applied for exergy calculations are presented. Finally, the methodology for exergy cost analysis is summarized.

2.1 System description

The system analyzed is depicted in Figure 1, and consists of five subsystems: solar loop, sanitary hot water (SHW) loop, membrane distillation (MD) module, reverse osmosis (RO) module and power loop. The solar loop includes four PVT collectors (1.63 m^2 each) divided in two sets (PVT 1-2 and PVT 3-4), as well as an evacuated tubes collector (ETC, of 3 m^2) and the pump needed for water-glycol circulation. SHW loop comprises a 325 L hot water tank (HWT) and the required pumps and valves to divert or mix the SHW according to scheduled temperatures. The membrane distillation is driven by hot water from the HWT trough a heat exchanger (HX-Tank MD in Figure 1). It is permeate gap module type (PGMD) and can produce up to 20 L/h at good irradiation conditions. The RO module produces 30 L/h and consumes 110 W in its constant operation. Finally, the power loop collects the power generated by the PVT collectors (4 x 240 W) and the micro wind turbine (WT, 400 W), which is stored in a two lead-acid batteries set (250 Ah and 12 V in serial), and consumed in pumps, RO and the domestic power demand. The system model was developed for the design of an experimental facility erected at the University of Zaragoza; for this reason, data of components corresponds to commercially available devices

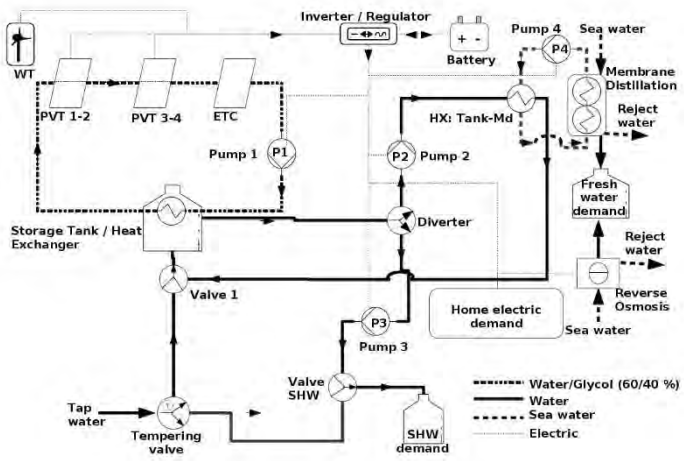

Figure 1: General structure of the trigeneration scheme.

2.2 System modeling

Hybrid trigeneration system has been modeled by TRNSYS. A detailed description of the model that led to the plant definite design can be found in a previous paper [52] that included an ad-hoc model of MD unit. Weather conditions of plant location (Zaragoza, Spain) have been obtained from Meteonorm database [53]. Demands of FW and SHW have been estimated as recommended in [54] and domestic power demand has been calculated according to Spanish patterns [55,56]. In order to simulate as much as possible the pilot unit operation, the plant control system was also implemented in TRNSYS:

- a hysteresis loop (7-2 ºC) to adequately supply thermal energy from the solar loop to the HWT,
- set point temperature to activate the MD (63 ºC),

- SHW is fixed at 60 ºC, and it is mixed with tap water depending on the HWT temperature,
- aerotherm (not included in Figure 1) is activated when the ETC or PVT outlet temperatures reached to 85 ºC and 80 ºC respectively to cool the solar loop.
- similar flow rates were included in the circulating pumps (400 L/h).

Besides, a 1000 L fresh water tank has been introduced to model FW demand consumption. So, RO plant is activated when water content falls below 500 L and is stopped when the amount of water reaches 1000 L.

Results of the simulation include the ten-minute evolution of matter and energy flows within the system during a year. This time step has been selected because it is the maximum time step in TRNSYS that validates the typical on-off operation of the solar pump when the sun is raising and setting every day.

2.3 Exergy analysis

Once flow rates, temperatures, power flows and other parameters have been obtained by TRNSYS, exergy flows were calculated by using a separated Excel spreadsheet. This software has been used because it allows one to implement easily formulae used for exergy cost calculation. Exergy of sun radiation is obtained by applying the well-known approach proposed by Petela [57]:

$$\dot{B}_{rad} = IA_a\left(1 + \frac{1}{3}\left(\frac{T_0}{T_s}\right)^4 - \frac{4}{3}\left(\frac{T_0}{T_s}\right)\right) \quad (1)$$

Where I is the solar intensity, A_a is the surface area, T_0 is the reference temperature and T_s is the temperature of surface emitting radiation (in K). It should be noted that the reference temperature for exergy calculations has been made equal to ambient temperature and, thus, varies along the year. In the case of wind, exergy is equal to kinetic energy multiplied times a factor related to Betz limit [58]:

$$\dot{B}_{wind} = 0.597 \cdot \frac{1}{2}\dot{m}v^2 = 0.597 \cdot \frac{1}{2}A\rho v^3 \quad (2)$$

Where ṁ is mass flow rate (of air, in this case), v is its velocity, A is its impingement area and ρ is the density. Physical exergy of water and water-glycol streams is calculated taking into account that TRNSYS does not consider explicitly pressure drops and assuming incompressible flow with constant specific heat:

$$\dot{B}_{ph} = \dot{m}\, c \left(T - T_0 - T_0 ln\left(\frac{T}{T_0}\right)\right) \quad (3)$$

c is the specific heat, T is the flow temperature, and T_0 is the reference temperature, both in K. Finally, specific chemical exergy of salt-water mixtures, is calculated by the following formula [59]:

$$b_{ch} = N_s R T_0 ln \frac{N_s}{N_s + \sum\left(\frac{\beta_i C_i}{\rho MW_i}\right)} \quad (4)$$

$$N_s = \frac{1000 - \sum\left(\frac{C_i}{\rho}\right)}{MW_s} \quad (5)$$

Where C_i is the weight concentration of the i^{th} component per liter of solution (g/L), MW_s and MW_i are the molecular weights of the solvent and i^{th} component,

respectively, and β_i is the number of particles generated by the dissociation of the i^{th} component in the solution. Fresh water produced by reverse osmosis has a salt averaged concentration of 300 mg/L; accordingly, its chemical exergy is equal to 2.563 kJ/kg. Fresh water from membrane distillation has a salt concentration of only 20 m/L, what yields a chemical exergy value of 2.685 kJ/kg. For exergy of water mixed from the two sources, an average exergy value of 2.587 kJ/kg is used. In order to put in context the previous figures, the maximum salt concentration for drinking water is around 1000 mg/L, with corresponds to an exergy value of 2.450 kJ/kg. Algthough physical exergy is considered in the analysis, freshwater produced is quite close to ambient temperature. Accordingly, including physical exergy does not affect calculated exergy efficiency of both RO and MD. Anyway, low exergy efficiencies will be expected due to the low recovery ratio (RC) of both modules (10% and 2% for RO and MD respectively). On the other hand, the term of physical exergy is relevant in hot water flows (actually, as it will be seen later, aggregated yearly exergy of hot water is higher than aggregated exergy of cold fresh water, despite of volume of the former is lower than that of the latter).

Once exergy flows have been calculated, the exergy efficiency of components is obtained by dividing exergy of product into exergy of fuel.

$$\eta_b = \frac{\dot{P}}{\dot{F}} \tag{6}$$

Besides, fuel minus product is equal to irreversibility:

$$\dot{I} = \dot{F} - \dot{P} \tag{7}$$

It should be noted that, sometimes, the product (and, accordingly, the efficiency) is equal to the summation of several terms; for instance, PVT panels have two products: increment in the exergy of water-glycol flow, and electricity. Besides, in transient operation, fuel and product of components with accumulation have to include a transient term.

It is also interesting to calculate aggregated values for a given period of time (e.g. one month), what can be done by integrating exergy flows along the considered time.

$$B = \int_{period} \dot{B} dt \quad (8)$$

In this case, efficiency and irreversibility become:

$$\eta_{b,av} = \frac{P}{F} \quad (9)$$

$$I = F - P \quad (10)$$

In order to apply exergy analysis, plant structure has been simplified and relevant components and exergy flows have been numbered (Figure 2). Component 1 is the wind turbine, whereas component 2 is the electricity management system (including batteries). PVT 1-2, PVT 3-4 and evacuated tube collectors correspond to components 3 to 5. An additional component (number 6) has been introduced in the solar loop to take into account heat loses in pipes, energy consumed by solar pump and, eventually, the heat dissipation system to avoid overheating. Component 7 is the sanitary hot water tank, and components 8 and 9 are respectively the membrane distillation unit (MD) and reverse osmosis unit (RO). A fresh water tank (component

11) stores fresh water from 8 and 9 to accommodate a daily demand of fresh water and to supply cold water to produce SHW in 7. Finally, component 10 is a mixer that consumes cold water from the tank 11 to reduce the SHW temperature service when it exceeds 60ºC from the tank 7. Flows 1 to 4 correspond to wind and solar exergy. Flows 5 to 10 are water-glycol streams of solar loop, whereas flows 11 to 19 are fresh water and SHW streams. Finally, 20 to 26 are electricity flows. It should be noted that sea water flows are not represented because they come from the environment (seawater) and, thus, have no exergy. Besides, brine flows are also not represented because they are useless streams that are being dissipated in the environment. This latter simplification is equivalent to include the irreversibility associated with this dissipation in the same control volume of the distillation facilities where are generated, in this way the analysis is not guided to the cost analysis of some residues that specifically provoke desalination facilities, that could be accounted for in other studies [60].

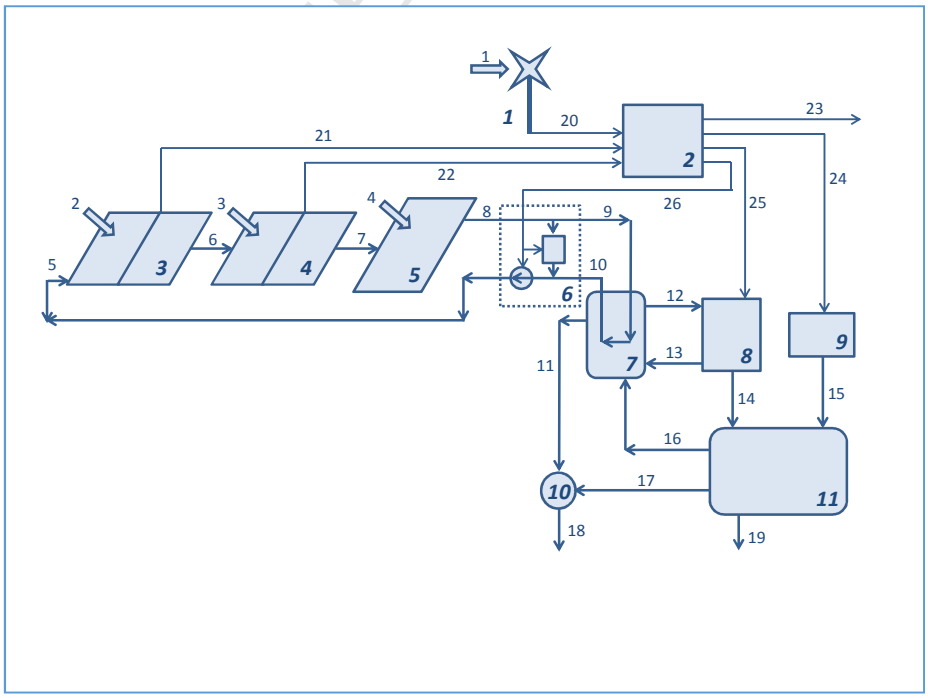

Figure 2: Flow and components of the trigeneration scheme.

Once flows and components have been defined and numbered, the fuel-product definition can be made. This definition is summarized in Table 1, where it can be seen that some components may have more than one fuel or more than one product (being the total equal to the summation of the different parts). For instance, PVT panels (components 3 and 4) have only one fuel (solar radiation) but two products (increment of exergy of water-glycol stream, and electricity). Besides, membrane distillation unit (component 8) and solar loop (component 6) consume both thermal exergy and electricity. An interesting issue appears in components where accumulation takes place: component 2 (due to batteries), 7 (hot water tank) and 11 (fresh water tank). When exergy accumulated in these component increases (e.g. temperature of HWT is increasing), this increment has to be part of the product; however, when stored exergy decreases, the absolute value of this reduction has to be part of the fuel. This issue has been introduced in the fuel definition y using the terms in brackets with a superscript "+", which means that when the term is positive, it has to be considered and when it is negative it has to be made equal to 0. Finally, besides all accumulation terms, the fuel of the whole plant includes solar energy and wind, whereas its product is made of three components: sanitary hot water, fresh water and electricity.

If instead of considering a given instant, the analysis is made by using aggregated values along a given period of time, fuel and product definition detailed in the table can also be used by introducing two changes: i) flow rates, $\dot{B}$, should be exergy flows, B, and ii) transient terms disappear (they become equal to the variation of exergy between the beginning and the end, which is negligible for long periods such as one month or one year. This situation allows one to apply conventional symbolic thermoeconomic methodology for exergy cost calculation.

Component	Fuel			Product		
1. WT	$\dot{B}_1$			$\dot{B}_{20}$		
2. Elec. control.	$\dot{B}_{20} + \dot{B}_{21} + \dot{B}_{22} + \left[-\frac{dB_{C2}}{dt}\right]^+$			$\dot{B}_{23} + \dot{B}_{24} + \dot{B}_{25} + \dot{B}_{26} + \left[\frac{dB_{C2}}{dt}\right]^+$		
3. PVT 1-2	$\dot{B}_2$			$\dot{B}_6 - \dot{B}_5$	$\dot{B}_{21}$	
4. PVT 3-4	$\dot{B}_3$			$\dot{B}_7 - \dot{B}_6$	$\dot{B}_{22}$	
5. ECT	$\dot{B}_4$			$\dot{B}_8 - \dot{B}_7$		
6. Solar loop	$\dot{B}_8 - \dot{B}_5$	$\dot{B}_{26}$		$\dot{B}_9 - \dot{B}_{10}$		
7. HWT	$\dot{B}_9 - \dot{B}_{10} + \left[-\frac{dB_{C7}}{dt}\right]^+$			$\dot{B}_{12} - \dot{B}_{13} + \dot{B}_{11} + \dot{B}_{16} + \left[\frac{dB_{C7}}{dt}\right]^+$		
8. MD	$\dot{B}_{12}$-$\dot{B}_{13}$	$\dot{B}_{25}$		$\dot{B}_{14}$		
9. RO	$\dot{B}_{24}$			$\dot{B}_{15}$		
10. Mixer	$\dot{B}_{11} + \dot{B}_{17}$			$\dot{B}_{18}$		
11. Tank	$\dot{B}_{14} + \dot{B}_{15} + \left[-\frac{dB_{C11}}{dt}\right]^+$			$\dot{B}_{16} + \dot{B}_{17} + \dot{B}_{19} + \left[\frac{dB_{C11}}{dt}\right]^+$		
TOTAL PLANT	$\dot{B}_2 + \dot{B}_3 + \dot{B}_4$	$\dot{B}_1$	$\left[-\frac{dB_{C2}}{dt}\right]^+ + \left[-\frac{dB_{C7}}{dt}\right]^+ + \left[-\frac{dB_{C11}}{dt}\right]^+$	$\dot{B}_{18} + \left[\frac{dB_{C7}}{dt}\right]^+$	$\dot{B}_{19} + \left[\frac{dB_{C11}}{dt}\right]^+$	$\dot{B}_{23} + \left[\frac{dB_{C2}}{dt}\right]^+$

Table 1: Fuel and product definition.

2.4 Exergy cost analysis

Exergy cost calculations will be made by applying symbolic thermoeconomics, which is a methodology for the analysis of energy systems based on Exergy Cost Theory and a compact formulation by matrix operators [43,44]. The main concept and formulae of the methodology are summarized below.

The system is represented by a productive structure that describes the purpose of the different components. This structure is composed of n components (plus component 0 which is the environment), each of them consumes resources from other components or from the environment (fuel, F), to produce useful effects for other components or for the environment (product, P). A flow that is part of the product of component i and becomes part of the fuel of component j is represented by E_{ij}. A table containing elements E_{ij} is the Fuel-Product table, and its definition is the first step for building a thermoeconomic model.

The exergy cost of a flow E_{ij} (indicated by E_{ij}^{*}) is the amount of exergy resources used to produce this flow. Exergy flow of fuel and product are represented by F* and P*, respectively. The unit exergy cost of a flow is the quotient between its exergy cost and its exergy and it is represented as k*.

Thermoeconomic model is based on distribution coefficients y_{ij}, which quantify the part of the product of the j^{th} component that becomes fuel of the i^{th} component:

$$y_{ij} = \frac{E_{ji}}{P_j} \tag{11}$$

A matrix containing elements y_{ij} is called $\langle \boldsymbol{FP} \rangle$.

In [44], a formulation of cost decomposition of stream into terms considering the irreversibility of different components was developed. It was demonstrated that, in a system without wastes, the vector containing exergy cost of the product of all plant components can be calculated as:

$$\boldsymbol{P}^{*} = \boldsymbol{P} + \left(\boldsymbol{U}_{\boldsymbol{D}} - \left\langle \boldsymbol{FP} \right\rangle\right)^{-1} \boldsymbol{I} \tag{12}$$

The previous equation indicates that the cost of the products is equal to its exergy plus additional terms due to irreversibility appearing in the different components. In an ideal process without irreversibility, the cost of all products would be equal to its exergy. However, since processes are real, the cost of product increases. Once exergy cost decomposition is calculated by applying eq. 12, unit cost decomposition is straightforward by dividing exergy cost into exergy. In this case, unit exergy cost is equal to 1 plus other terms caused by irreversibility of plant components located upstream in the cost formation process.

In [45], a different approach for the decomposition of cost is proposed. It is based on the origin of resources consumed by the system, which is interesting in the example analyzed in this paper that consumes both wind and solar energy.

The first step is to decompose the vector of fuel consumed by the plant into a summation of n_f terms, each one corresponding to a different kind of energy (e. g. sun and wind):

$$\boldsymbol{F}_{\boldsymbol{e}} = \sum_{k=1}^{n_f} {}^{k}\boldsymbol{F}_{\boldsymbol{e}} \tag{13}$$

With this fuel decomposition, in [45] it was shown that cost of product of all plant components can also be decomposed as:

$$\boldsymbol{P}^{*} = \sum_{k=1}^{n_f} {}^{k}\boldsymbol{P}^{*} \tag{14}$$

where:

$$ {}^{k}\boldsymbol{P}^{*} = \left(\boldsymbol{U}_{\boldsymbol{D}} - \left\langle \boldsymbol{FP} \right\rangle\right)^{-1} {}^{k}\boldsymbol{F}_{\boldsymbol{e}} \quad (15) $$

Like in the decomposition of exergy cost presented in eq. 12, unit exergy cost decomposition can be obtained by dividing exergy cost into exergy.

In order to apply the symbolic thermoeconomic formulation for exergy cost calculation, Fuel - Product table containing values of flows E_{ij} has to be defined. This definition appears in Table 2 as function of exergy values of the different flows. Each row of the table shows how the product of a given component becomes part of the fuel of other components or part of the total plant product. Besides, each column corresponds to the fuel of a component, which comes either from other components or from the environment (component 0). The summation by rows indicates the total product of a component, whereas the summation by columns indicates its total fuel. It can be seen that these total products and fuels are equal to the ones defined previously.

	F1	F2	F3	F4	F5	F6	F7	F8	F9	F10	F11	Plant prod.	Total Product
P 0. Env.	B_1	0	B_2	B_3	B_4	0	0	0	0	0	0	0	$B_1+B_2+B_3+B_4$
P1. WT	0	B_{20}	0	0	0	0	0	0	0	0	0	0	B_{20}
P2. Elec. cont.	0	0	0	0	0	B_{26}	0	B_{25}	B_{24}	0	0	B_{23}	$B_{23}+B_{24}+B_{25}+B_{26}$
P3. PVT 1-2	0	B_{21}	0	0	0	B_6-B_5	0	0	0	0	0	0	$B_6-B_5+B_{21}$
P4. PVT 3-4	0	B_{22}	0	0	0	B_7-B_6	0	0	0	0	0	0	$B_7-B_6+B_{22}$
P5. ETC	0	0	0	0	0	B_8-B_7	0	0	0	0	0	0	$B_8–B_7$
P6. Solar loop	0	0	0	0	0	0	B_9-B_{10}	0	0	0	0	0	$B_9–B_{10}$
P7. HWT	0	0	0	0	0	0	0	$B_{12}-B_{13}$	0	$B_{11}-B_{16}$	0	0	$B_{12}–B_{13}+B_{11}–B_{16}$
P8. MD	0	0	0	0	0	0	0	0	0	0	B_{14}	0	B_{14}
P9. RO	0	0	0	0	0	0	0	0	0	0	B_{15}	0	B_{15}
P10. Mixer	0	0	0	0	0	0	0	0	0	0	0	B_{18}	B_{18}
P11. Tank	0	0	0	0	0	0	0	0	0	$B_{16}+B_{17}$	0	B_{19}	$B_{16}+B_{17}+B_{19}$
Total fuel	B_1	$B_{20}+B_{21}+B_{22}$	B_2	B_3	B_4	$B_{26}+B_8-B_5$	B_9-B_{10}	$B_{25}+B_{12}-B_{13}$	B_{24}	$B_{11}+B_{17}$	$B_{14}+B_{15}$	$B_{18}+B_{19}+B_{23}$	

Table 2: Generic F-P table.

3. Results and discussion

The aim of this section is to present the main results of the application of exergy and exergy cost analyses previously presented to the renewable energy-based polygeneration plant. First of all, exergy analysis has been applied to the base case by considering two time scales: detailed time evolution of selected days (ten minutes basis) and aggregated values (monthly basis). Afterwards, exergy cost analysis is applied for aggregated values (monthly and yearly). Finally, exergy and exergy cost analyses are applied to the assessment of three variations of the base case. Note that neither exergy efficiency nor exergy cost analysis could be compared with any other similar installation due to the differences in the arrangement and size presented in the introductory section.

3.1 Detailed time evolution

Figure 3 shows the time evolution of product, fuel and efficiency of the first set of PVT panels during a selected winter day (30th January). The fuel is the exergy of solar radiation (obtained from data by Meteonorm database [53] for Zaragoza), whereas the product is composed of two parts: the increment of exergy of water-glycol heated in the collector and electricity produced. It can be clearly seen how both fuel and product, are higher during the central hours. Besides, the main part of the product is electricity production because exergy of heated water-glycol is much lower than its energy.

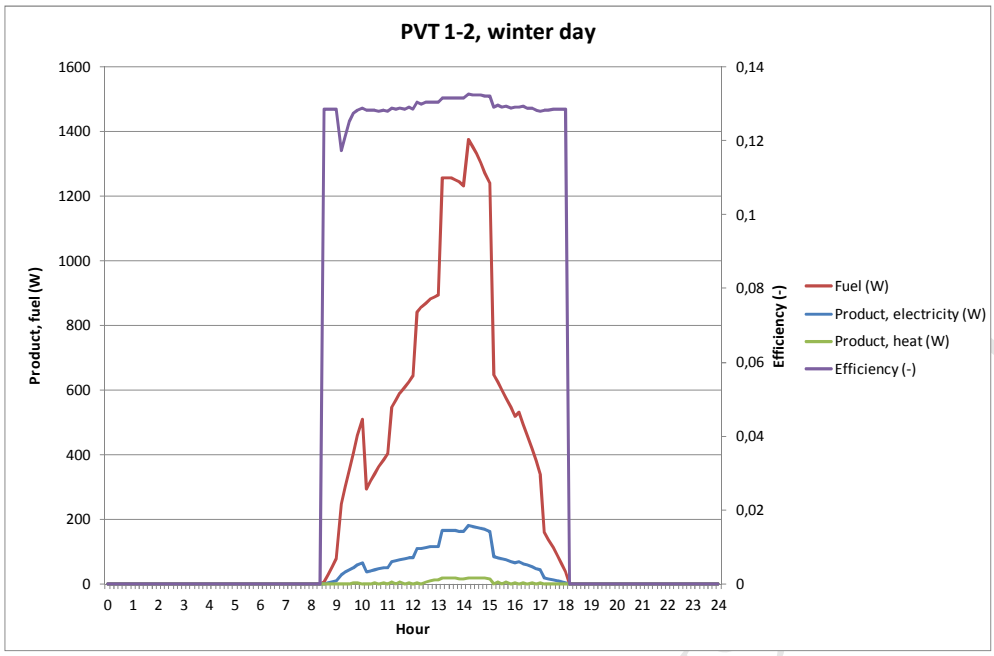

Figure 3: Time evolution of exergy fuel, product and efficiency of PVT collector in an example winter day.

Fuel, product and efficiency of evacuated tube collector for a selected summer day (19th July or the 200th day of the year) is plotted in Figure 4. It can be seen how this collector presents lower efficiency, because it produces only heat. Besides, some peaks appear due to the control that activates or not the water-glycol pump in the short periods when the sun rises and sets every day.

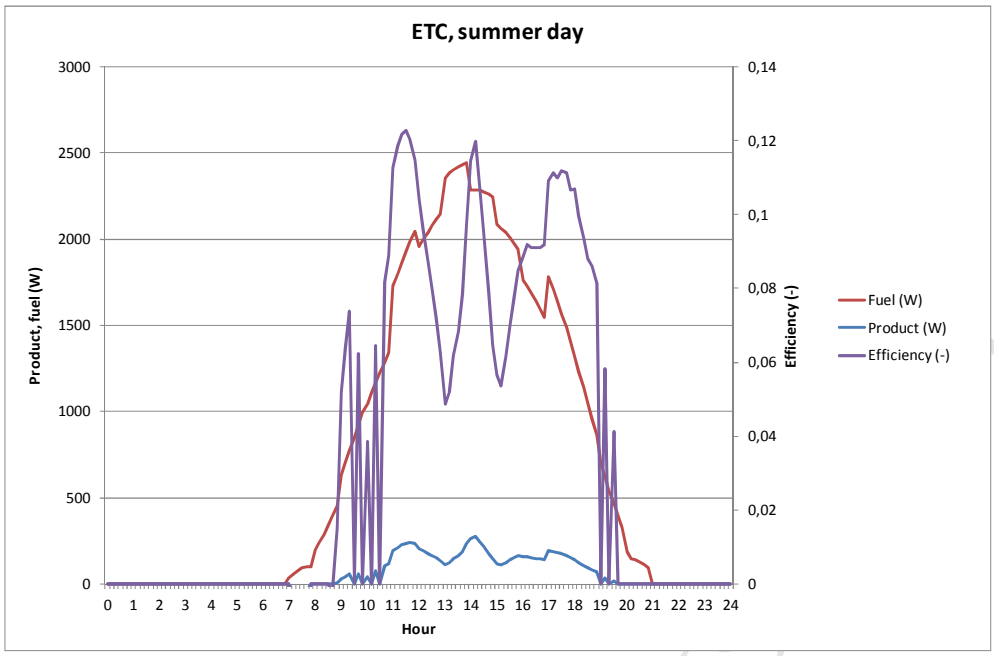

Figure 4: Time evolution of exergy fuel, product and efficiency of evacuated tube collector in an example summer day.

A similar graph for wind turbine for 30th January is depicted in Figure 5. In this case, the time evolution of the variables is strongly dependent on the day; for the chosen example, wind blows at night, morning and evening, but not in the afternoon. This fact can be seen by considering that exergy of wind is proportional to wind speed raised to the third power. Besides, efficiency is quite constant except when wind velocity is below the minimum for turbine connection or above a given value when power does not increase despite of higher wind speed. This can be explained by the typical power / wind speed curve that characterizes a wind turbine and is available in TRNSYS: for low speed, power increases smoothly, afterwards, curve slope increases and, finally, at a given speed, power decreases sharply.

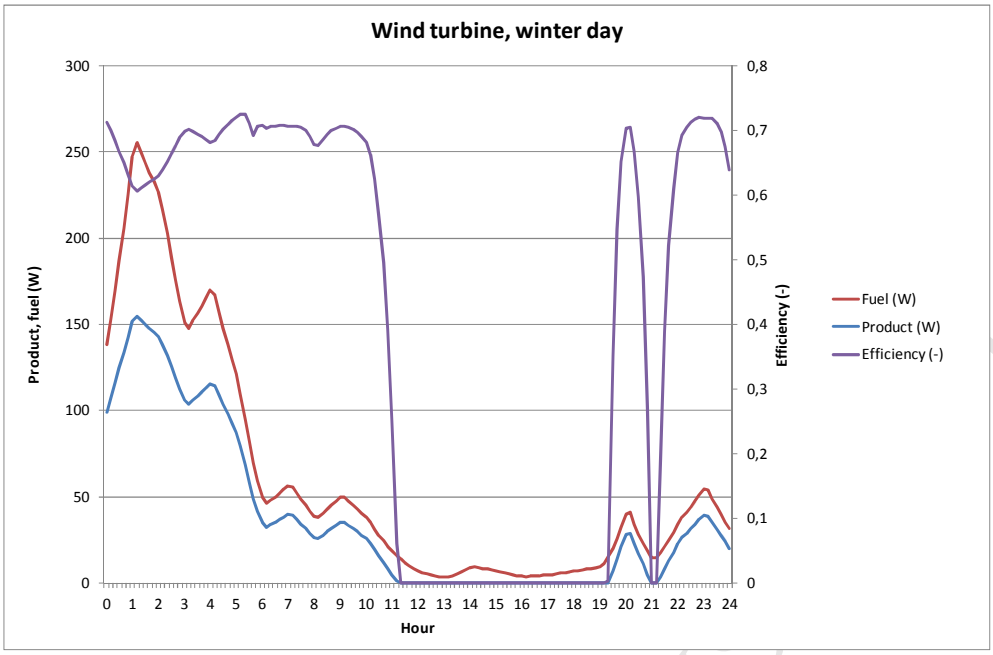

Figure 5: Time evolution of exergy fuel, product and efficiency of wind turbine in an example winter day.

3.2 Aggregated monthly analysis

The analysis presented in the previous section is interesting for observing details of system behavior. However, in order to assess global system efficiency, it is more convenient to apply aggregated variables, for instance, in monthly basis. This analysis appears in Figure 6 for the first set of PVT panels. Bars in the graph show how the exergy of fuel (total bar length) is either transformed into useful products (electricity and heat) or destroyed (irreversibility). It should be noted that, due to the time integration, now fuel, products and irreversibility appear not in power units but in energy units (MJ). Aggregated efficiency is represented by a line. It can be seen how the higher values of efficiency appear not in summer but in spring and autumn. This effect is due to the fact that efficiency is affected by two different causes: on one side,

hot ambient temperatures reduce thermal losses, but also reduce production of electricity. Figure 7 shows the same graph but for evacuated tube collectors (ETC). It can be seen how lower efficiency appears in autumn and winter due to higher losses and also lower temperature of heated water (lower ratio exergy/energy); besides, its efficiency is much lower than that of the PVT panels. It should be highlighted that the use of exergy allows one to include power and heat in the same graph but taking into account the different thermodynamic qualities of both flows.

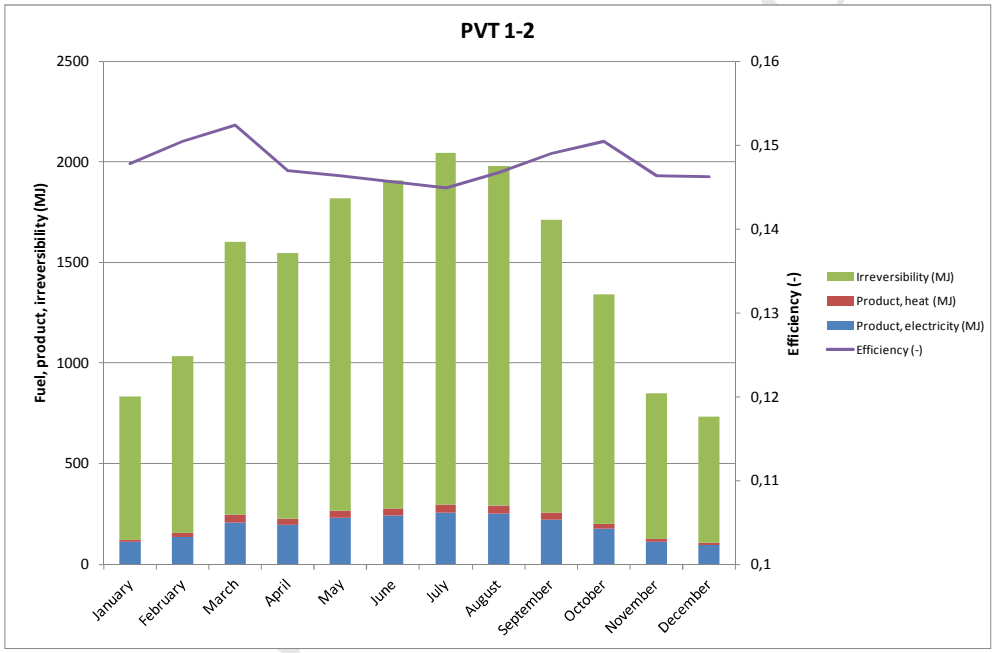

Figure 6: Aggregated monthly exergy analysis: fuel, product, irreversibility and efficiency of PVT collector 1-2.

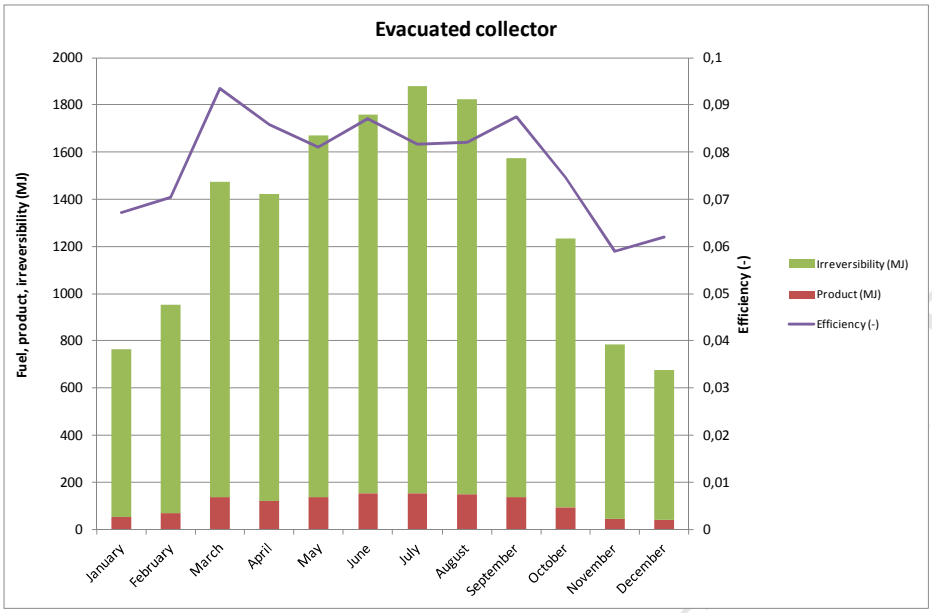

Figure 7: Aggregated monthly exergy analysis: fuel, product, irreversibility and efficiency of evacuated tubes collector.

Water-glycol loop (component 6) is analyzed in Figure 8. It includes pump, loses in pipes and, eventually, heat dissipation for avoiding overheating. It can be seen that efficiency is lower in winter because then the relative importance of electric pump consumption is higher.

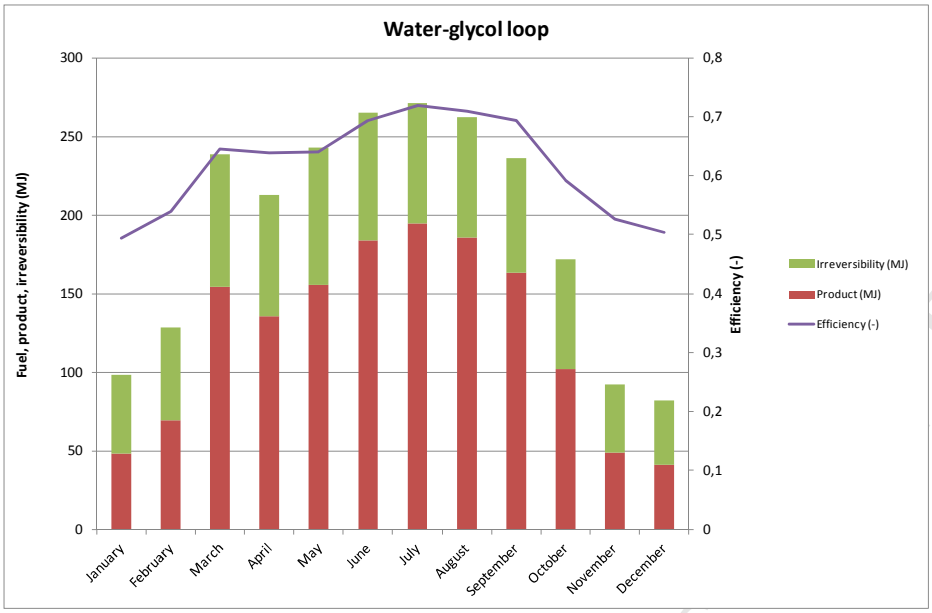

Figure 8: Aggregated monthly exergy analysis: fuel, product, irreversibility and efficiency of water-glycol loop.

Behavior of hot water tank is represented in Figure 9. Efficiency of this component varies from 25 to 45%, being usually lower in hotter months. This fact can be explained by taking into account that higher ambient temperatures means lower thermal loses but also higher irreversibility in the heat transfer from hot water-glycol from the thermal collectors (at higher temperatures) to SHW stored in the tank.

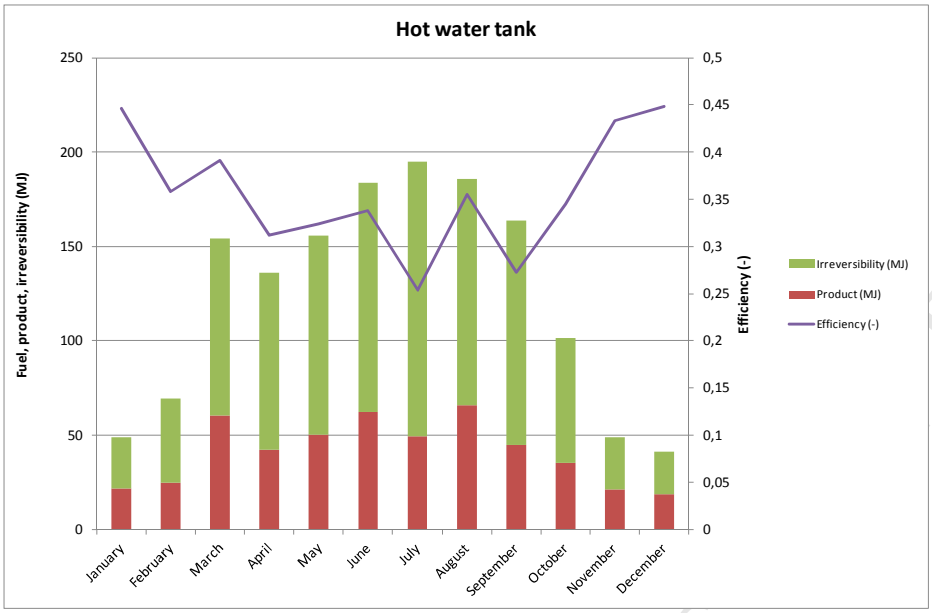

Figure 9: Aggregated monthly exergy analysis: fuel, product, irreversibility and efficiency of hot water tank.

Fuel, product, irreversibility and efficiency of membrane distillation unit are plotted in Figure 10. It can be seen that this unit only can operate in sunny days and hot months, and requires heat but also power for pumping seawater and SHW flows. However, its efficiency is higher in winter sunny days because the lower temperature of the feeding seawater tank compensates the lower temperature obtained in the SHW tank (note that the driving force to distillate in a MD is the temperature drop between the hot energy source and cold seawater feed). In general, efficiency is quite low, what makes it only interesting when it is properly integrated with a low temperature heat source. Finally behavior of reverse osmosis unit appears in Figure 11. This desalination technology has higher efficiency and it is bigger in summer since higher seawater feeding temperatures lead to lower specific power consumption in the RO membranes. It should be noted that due to the use of exergy, flows of different nature (hot water, electricity and fresh water) can be quantified in

the same units and, thus, thermodynamic efficiency of desalination technologies can be calculated.

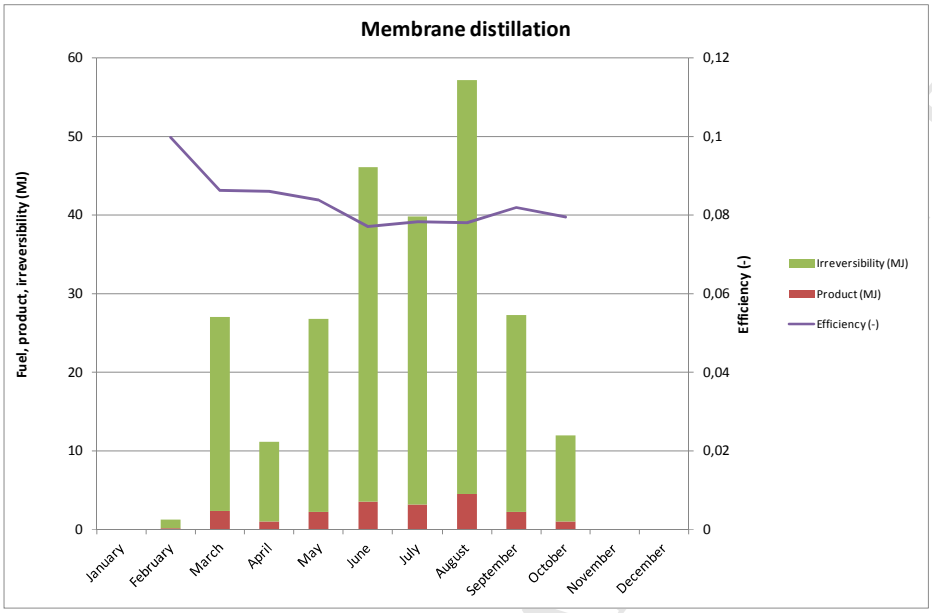

Figure 10: Aggregated monthly exergy analysis: fuel, product, irreversibility and efficiency of membrane distillation unit.

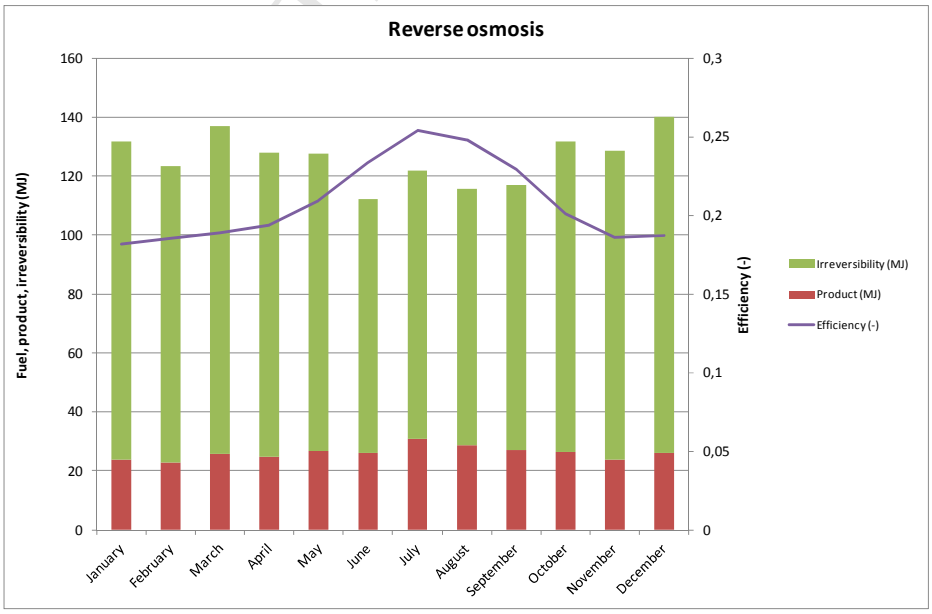

Figure 11: Aggregated monthly exergy analysis: fuel, product, irreversibility and efficiency of reverse osmosis unit.

Once exergetic parameters of the main individual components have been analyzed, the complete plant is considered. Figure 12 shows how, in each month, the total fuel entering the plant is transformed into products and irreversibilities of the plant components. The product with highest exergy is electricity, whereas contribution of hot water is small and effect of fresh water is negligible. Main irreversibilities appear in solar collectors. It can be seen how both fuel (total bar length) and product are bigger in hot months. In Figure 13, the contribution of each one of the plant fuels is represented. It can be seen that the most relevant resource is solar energy. Finally, plant efficiency is plotted in Figure 14, where it can be seen how the total efficiency is equal to the contribution of efficiency of electricity production, of fresh water production and of hot water production. The main contribution is due to electricity, as it can be expected because it is the main product. Efficiencies related to water are higher in cold months when a major contribution of reverse osmosis is found; its better efficiency will be analyzed in detail in next section.

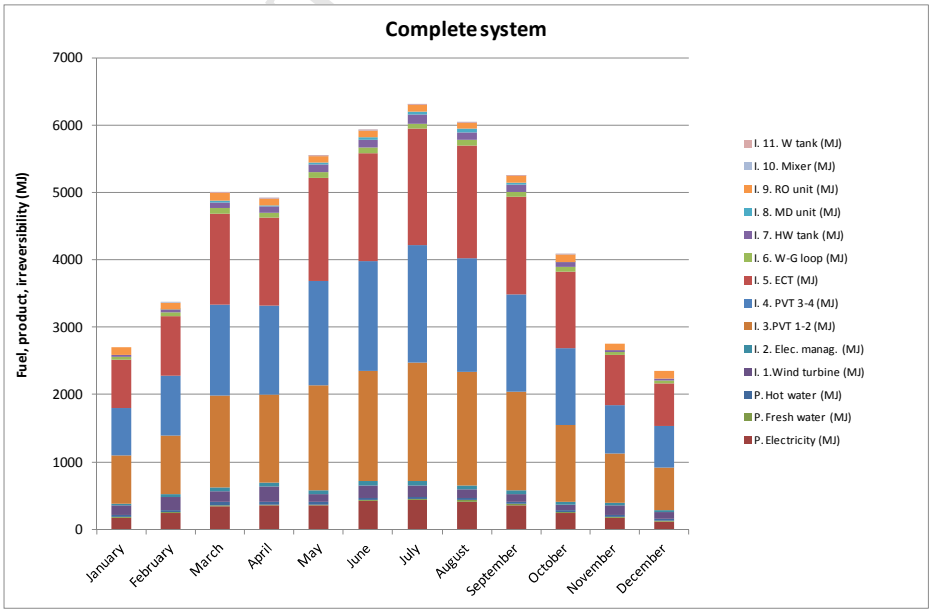

Figure 12: Aggregated monthly exergy analysis: fuel, product, irreversibility of the whole plant.

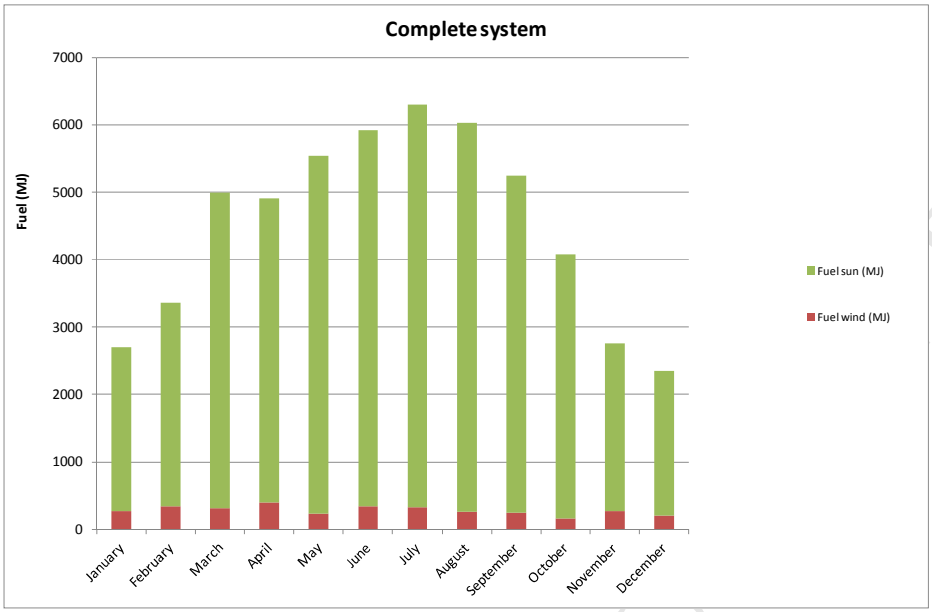

Figure 13: Aggregated monthly exergy analysis: fuel decomposition (solar and wind) of the whole plant.

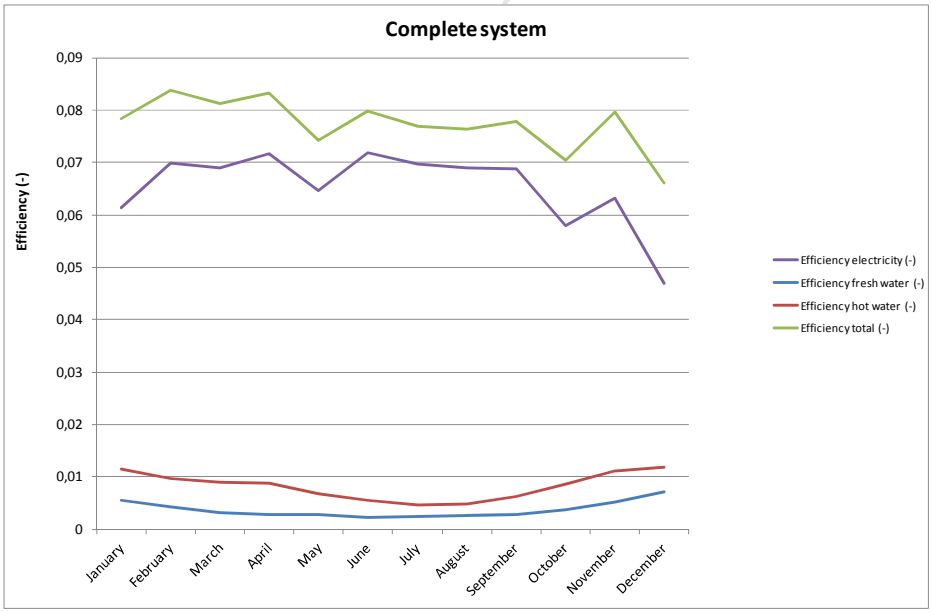

Figure 14: Aggregated monthly efficiency of the whole plant.

3.3 Exergy cost analysis

Exergy analysis presented in the previous section has allowed one to quantify efficiency and irreversibility of plant components and of the whole plant. However, exergy cost analysis allows one to go a step further by calculating the amount of resources required for producing the product of each component, in other words, its cost. Besides, it is possible to analyze in detail the process of formation of this cost in two ways: according to irreversibilities and tracing the origin of resources. This additional information can be relevant for detecting potentials of improvement.

Table 3 shows the unit exergy cost formation process according to irreversibility of the product of all plant components for the whole year. In the first column after the name of the devices, it can be seen the unit exergy cost of their products. These costs vary from the low values of efficient devices located at the beginning of the production chain, up to high values of products located at the end of this chain. The most relevant of the latest is fresh water produced by membrane distillation. The other columns represent how this cost is formed according to irreversibilities: It can be checked that for each device (each row) their summation is equal to the total unit exergy cost. If all plant components were ideal, all unit exergy cost would be equal to 1, which appear in the first column. The other 11 columns correspond to all plant components. Each element is affected by its own irreversibility and by irreversibilities of components located upstream in the productive chain. For example, wind turbine and solar collectors only have non-zero values in its own column; among these elements, evacuated tube collector is the less efficient and, accordingly, its product has the highest unit exergy cost. On the other hand, the product of water mixer (SHW, 10) is affected by irreversibilities of all components. Unit exergy cost of fresh water produced by membrane distillation is almost 18 times higher than the cost of

water produced by reverse osmosis; this factor comes from the inefficient MD process but also from its fuel (heat from solar field) that has followed a long production chain (collectors, water-glycol loop and water tank), what increases its exergy cost. This leads to a relevant conclusion: for improving efficiency, it would be interesting to reduce the length of this chain, for instance, by linking directly flow 9 to flow 12 and by reducing loses in the ducts connecting the solar panels with the SHW tank. If the table is observed by columns, the effect of the irreversibility of each component on the costs of other components can be seen. For example, irreversibility of evacuated tube collector (I5) has strong effect not only in the cost of its product but also in the cost of the products of components located downstream. This shows clearly that it is more advantageous from the efficiency point of view to use PVT collectors, although it is clear that ETC had to be introduced in order to achieve the level temperature to drive the MD unit.

	Total unit exergy cost	Ideal	I1	I2	I3	I4	I5	I6	I7	I8	I9	I10	I11
P1. WT	**2.07**	1	1.07	0	0	0	0	0	0	0	0	0	0
P2. Elec.cont.	**6.12**	1	0.32	0.11	2.36	2.33	0	0	0	0	0	0	0
P3. PVT 1-2	**6.77**	1	0	0	5.77	0	0	0	0	0	0	0	0
P4. PVT 3-4	**6.72**	1	0	0	0	5.72	0	0	0	0	0	0	0
P5. ETC	**12.44**	1	0	0	0	0	11.4	0	0	0	0	0	0
P6. Solar loop	**15.27**	1	0.07	0.02	1.82	1.88	9.93	0.55	0	0	0	0	0
P7. HWT	**45.63**	1	0.20	0.72	5.43	5.63	29.7	1.65	1.99	0	0	0	0
P8. MD	**531.6**	1	2.64	0.93	64.7	67.0	341.0	19.0	22.9	11.4	0	0	0
P9. RO	**29.58**	1	1.53	0.54	11.4	11.3	0	0	0	0	3.83	0	0
P10. Mixer	**51.47**	1	0.71	0.25	8.84	8.99	26.8	1.49	1.80	0.25	1.31	0.01	0.01
P11. Tank	**61.08**	1	1.63	0.57	14.9	15.0	21.0	1.17	1.40	0.70	3.69	0	0.02

Table 3: Unit exergy cost decomposition according to irreversibilities for the complete year.

Table 4 shows the unit exergy cost decomposition according to the consumed resource. It can be seen how sun has much more relevance that wind, especially in the thermal energy and water production part. Elements located at the beginning of the production chain only have a single contribution (wind for the wind turbine, and sun for the collectors).

	Total unit exergy cost	Sun	Wind
P1. WT	**2.07**	0	2.07
P2. Elec.cont.	**6.12**	5.51	0.61
P3. PVT 1-2	**6.77**	6.77	0
P4. PVT 3-4	**6.72**	6.72	0
P5. ETC	**12.44**	12.44	0
P6. Solar loop	**15.28**	15.15	0.13
P7. HWT	**45.63**	45.24	0.39
P8. MD	**531.64**	526.55	5.10
P9. RO	**29.58**	26.63	2.95
P10. Mixer	**51.47**	50.10	1.38
P11. Tank	**61.08**	57.93	3.15

Table 4: Unit exergy cost decomposition according to external fuel for the complete year.

Besides the cost formation process considering the whole year, it is interesting to analyze its evolution along the different months. In order to avoid an excess of detail, only the cost of the final plant products will be shown: electricity (product of 2), fresh water (product of 11) and hot water (product of 10).

Figure 15 shows the unit exergy cost formation process of electricity along the year. It can be seen how this cost is affected only by components 1 to 4, which are the only present in its productive chain. PVT panels have the lowest efficiency and have the highest impact on cost. Cost is slightly higher in summer because of two reasons:

first, the contribution of wind (more efficient) is lower; second, the efficiency of PVT panels is reduced by its operating (cell) temperature. Decomposition of unit exergy cost of electricity according to resources is plotted in Figure 16, where it can be seen how the contribution of wind is higher in winter but always smaller than that of sun.

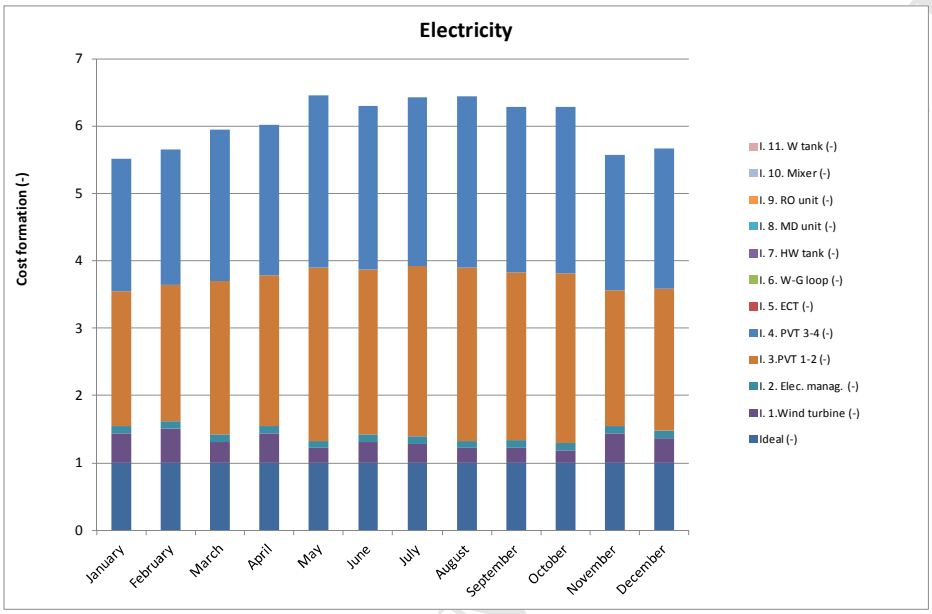

Figure 15: Unit exergy cost formation process of electricity according to irreversibility.

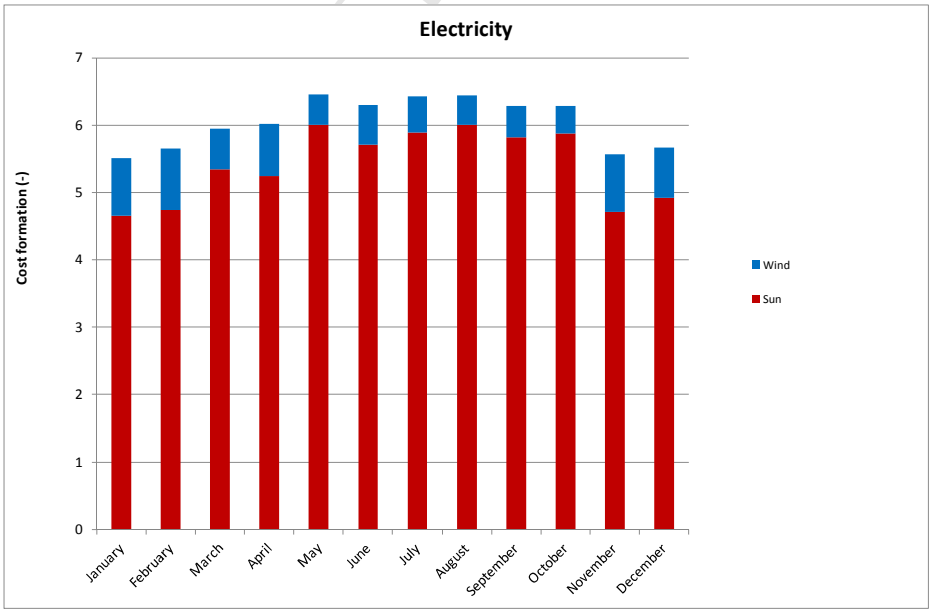

Figure 16: Unit exergy cost formation process of electricity according to resources.

The unit exergy cost formation of fresh water (product of 11) is analyzed in Figure 17 from the irreversibility point of view. It can be seen that the cost is much lower in cold months when most water (or even all water) is produced more efficiently by reverse osmosis. The most relevant contribution to this cost is that of solar panels, especially evacuated tube collector (what does not appear in cold months when no fresh water is distilled by MD). Figure 18 shows how the wind contribution is very low compared to solar energy.

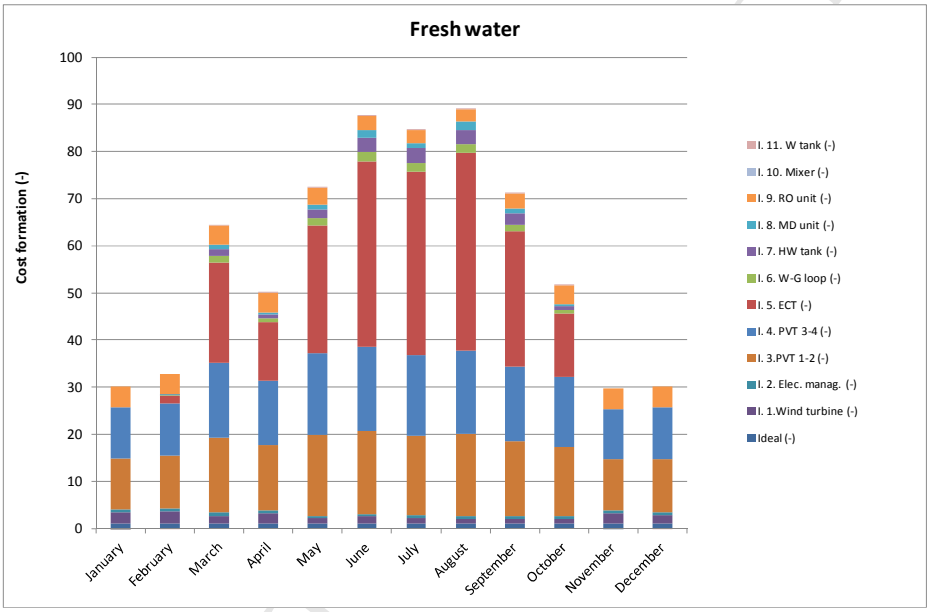

Figure 17: Unit exergy cost formation process of fresh water according to irreversibility.

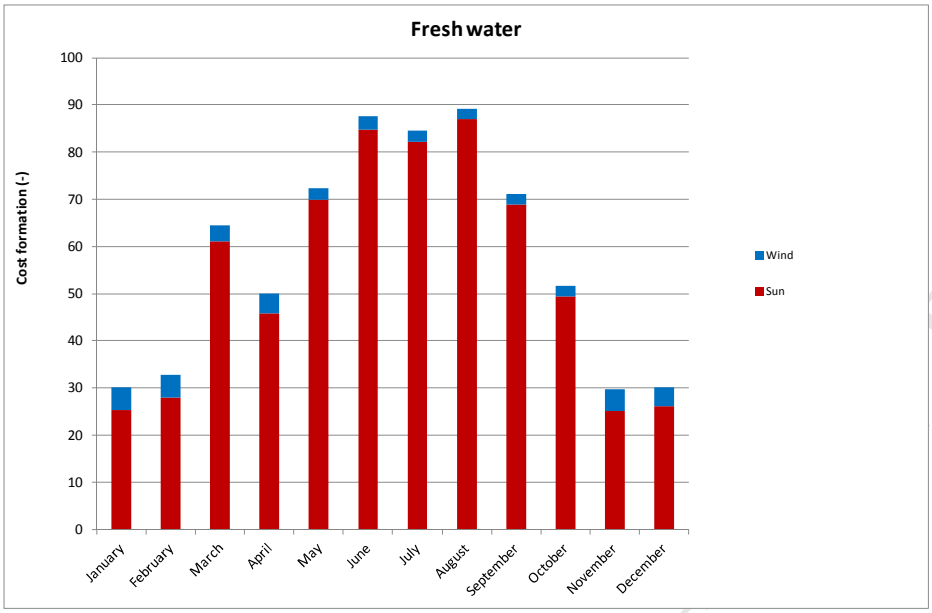

Figure 18: Cost formation process of fresh water according to resources.

Figure 19 shows the unit exergy cost formation process for SHW. It can be seen how this cost is clearly higher in summer than in winter: firstly, the cost of fresh water is higher and, secondly, specific thermal exergy of water decreases in summer because reference temperature (ambient temperature) increases as well. It can be seen how the main contribution is due to collectors, especially the evacuated tube. An interesting point is that unit exergy cost of hot water may be lower than cost of fresh water. This effect is explained by the fact that hot water requires two resources, fresh water and heat, and the unit exergy cost of the latter is significantly lower (see the unit exergy cost of the product of 6 and 7 in Table 3). Finally, in Figure 20 it can be seen the low contribution of wind energy in the cost formation of this plant product.

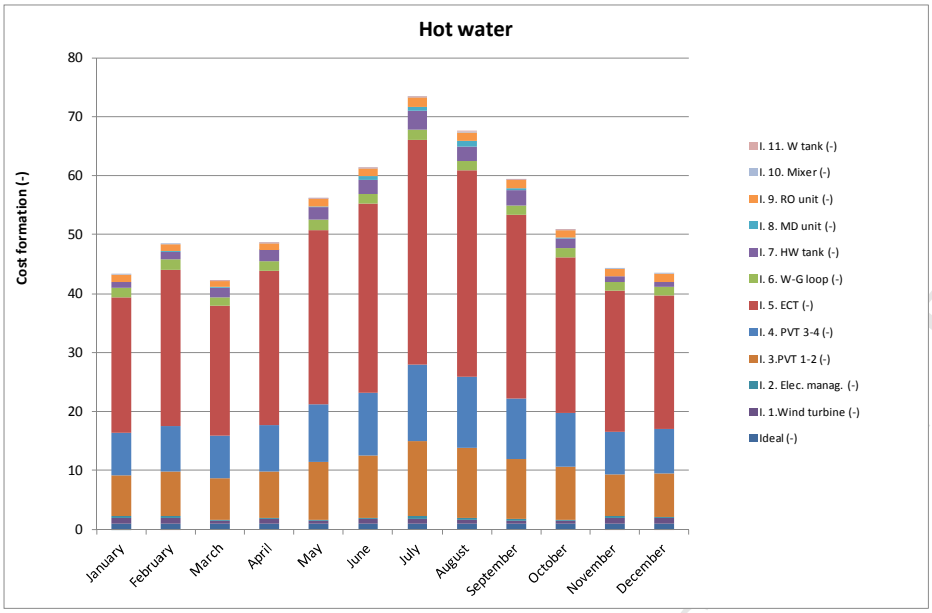

Figure 19: Unit exergy cost formation process of hot water according to irreversibility.

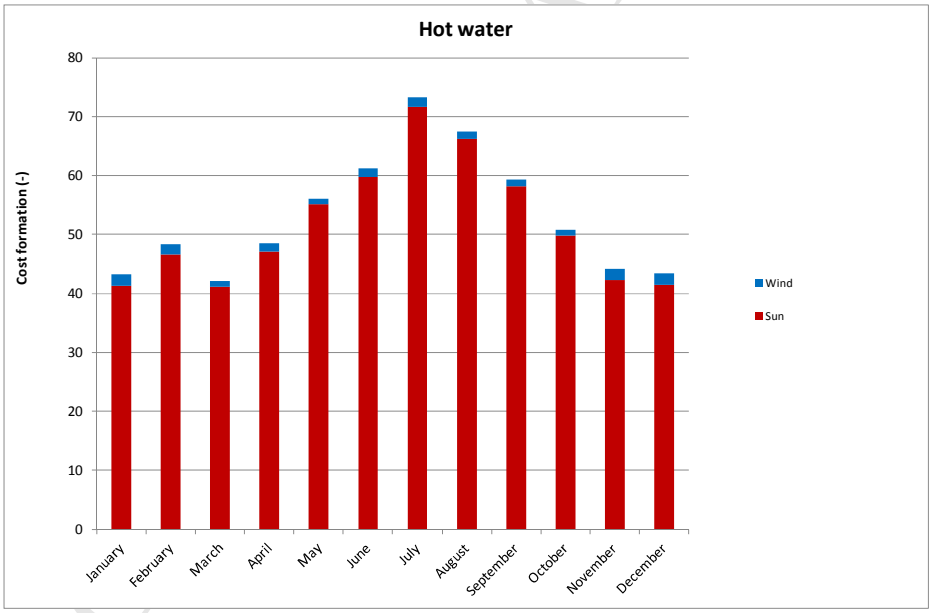

Figure 20: Unit exergy cost formation process of hot water according to resources.

3.4 Suggestions and assessment of plant modifications.

The analysis performed provides an in depth knowledge of the system from the exergy point of view (consumption of different resources, production of different flows

and efficiency). Accordingly, it allows to detect potential for improving system design. Although this improvement is a complex issue that not only considers efficiency, consumption of resources and plant production, but also other issues (e.g. economic investment, availability of resources, technological development and ability of the system to fulfill the demands in an isolated environment) identification of opportunities for energy savings and plant production and consumption may be a valuable first step (that later can be evaluated by considering the aforementioned issues).

The first relevant result is that global system exergy efficiency around 8% is a good figure, considering the scale of the system, the diversity of the products, and its ability to fulfill the demand during the year. Besides, the analysis shows that the weak part regarding efficiency is related to the “thermal branch” of the plant. In particular, evacuated tube collector has a strong impact on the unit exergy cost of components located downstream. This fact can be understood in two ways: on one hand, it would be interesting to reduce the relevance of this component, which is difficult because it is needed for increasing temperature up to a level suitable for driving MD unit; on the other hand, it confirms the positive effects of using PVT panels (with conventional thermal panels the efficiency would be much lower). Another relevant result is the very high unit exergy cost of fresh water produced by the MD unit, which appears partly because of its low efficiency and partly because of the long exergy transformation chain. This chain could be reduced by connecting directly the hot water demand of this device to the primary loop (avoiding the tank); this would improve efficiency and also water production by MD [7]. Finally, heat losses in pipes, pump and aerotherm in the solar loop or water-glycol loop (component 6) and electricity consumed by pumps and aerotherm in that component induces a non-negligible cost on fresh water and SHW. This impact would be reduced by increasing

the efficiency of that component. As an example, in the first plant modification case it has been simulated that electricity consumption of this component is reduced by 30%.

Related to the long and quite inefficient “thermal branch” explained above, is the low production of membrane distillation unit. In order to increase this production, a second modification of the plant will be the increment of ECT surface from 3 to 4.5 m^2.

Finally, it has been observed that the contribution of wind energy is low compared to the contribution of solar energy. For this reason, another plant modification consisting on replacing the 400 W wind turbine with a turbine of 800 W is also analyzed.

Monthly fresh water produced by MD unit for the four plant designs considered (base case, 4.5 m2 ECT, wind turbine of double size and improved solar loop) is represented in Figure 21. It can be seen how the increment of ECT size affects strongly this production, what is constant for the other three plant designs.

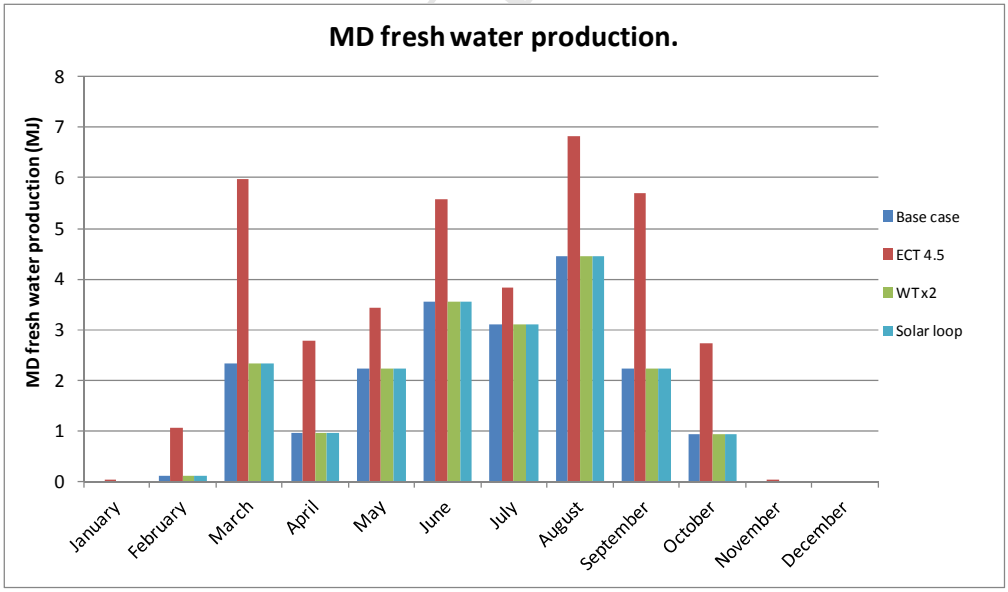

Figure 21: Exergy of fresh water produced by MD for the four cases analyzed.

Figure 22 shows how the increment of wind turbine size increases significantly plant electricity production. Besides, effect of electricity consumption of solar loop is no negligible, what points out the importance of ducts and ancillary pumps in efficiency of these systems. Finally, effect of increment of ECT size is small and depends on the month because of two effects: on one side, it increases MD fresh water production, what reduces electricity consumed by MD. On the other side, it increases the temperature of the water-glycol, what affects negatively the electricity produced by PVT.

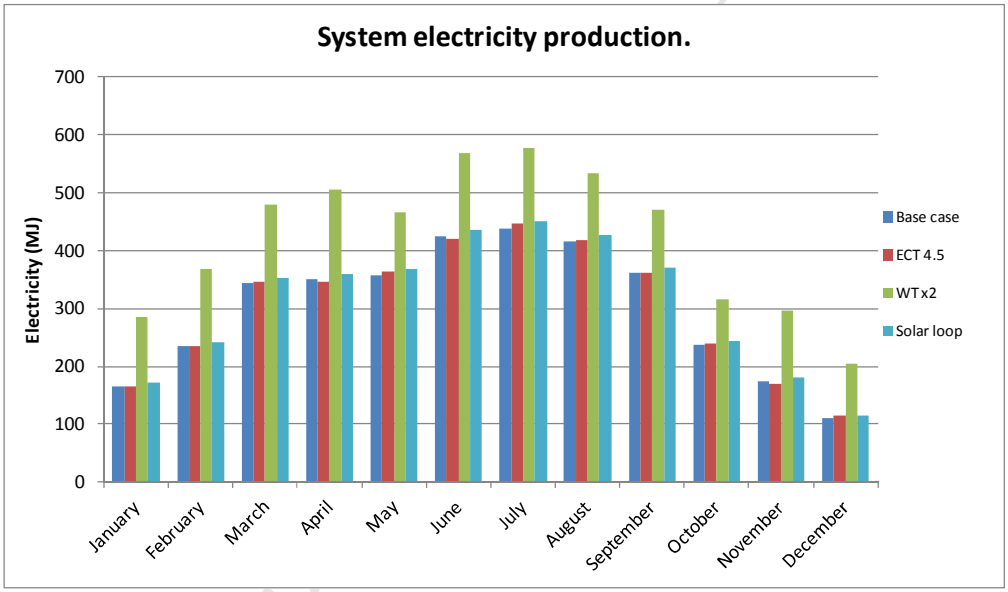

Figure 22: Net electricity produced by the plant for the four cases analyzed.

Table 5 shows the unit exergy cost of the product of plant components and its decomposition according to irreversibility for the case of ECT of 4.5 m^2. Unit exergy cost decomposition according to resources for the same case appears in Table 6. It can be seen how, compared to the base case, the unit exergy cost of ECT and components located downstream (solar loop, hot water tank and MD) decrease,

because efficiency of ECT increases due to the higher temperature of its product. On the other hand, since the fraction of fresh water produced by MD increases, and its cost is higher than fresh water produced by RO, costs of fresh and hot water clearly increase.

	Total unit exergy cost	Ideal	I1	I2	I3	I4	I5	I6	I7	I8	I9	I10	I11
P1. WT	**2.07**	1	1.07	0	0	0	0	0	0	0	0	0	0
P2. Elec.cont.	**6.09**	1	0.32	0.11	2.35	2.33	0	0	0	0	0	0	0
P3. PVT 1-2	**6.74**	1	0	0	5.74	0	0	0	0	0	0	0	0
P4. PVT 3-4	**6.69**	1	0	0	0	5.69	0	0	0	0	0	0	0
P5. ETC	**11.71**	1	0	0	0	0	10.71	0	0	0	0	0	0
P6. Solar loop	**14.15**	1	0.05	0.02	1.27	1.31	10.1	0.42	0	0	0	0	0
P7. HWT	**42.49**	1	0.14	0.05	3.81	3.94	30.3	1.26	2.00	0	0	0	0
P8. MD	**485.9**	1	1.87	0.66	45.1	46.5	342.7	14.3	22.7	11.1	0	0	0
P9. RO	**29.53**	1	1.53	0.54	11.4	11.3	0	0	0	0	3.85	0	0
P10. Mixer	**56.93**	1	0.65	0.23	7.90	8.00	33.8	1.41	2.24	0.43	1.20	0.01	0.02
P11. Tank	**84.94**	1	1.66	0.59	16.0	16.1	40.2	1.68	2.66	1.31	3.63	0	0.06

Table 5: Unit exergy cost decomposition according to irreversibilities for the complete year. Case with ECT of 4.5 m^2.

	Total unit exergy cost	Sun	Wind
P1. WT	**2.07**	0	2.07
P2. Elec.cont.	**6.09**	5.48	0.61
P3. PVT 1-2	**6.74**	6.74	0
P4. PVT 3-4	**6.69**	6.69	0
P5. ETC	**11.71**	11.71	0
P6. Solar loop	**14.15**	14.05	0.09
P7. HWT	**42.49**	42.21	0.28
P8. MD	**485.9**	482.3	3.61
P9. RO	**29.53**	26.57	2.96
P10. Mixer	**56.93**	55.68	1.25
P11. Tank	**84.93**	81.72	3.22

Table 6: Unit exergy cost decomposition according to external fuel for the complete year. Case with ECT of 4.5 m^2.

Unit exergy cost and its decomposition according to irreversibility for the case of bigger wind turbine appear in Table 7. Since it is more efficient than PVT, unit exergy cost of electricity (component 2) decreases and, accordingly, the cost of all components that consume electricity also does. However, this latter effect is negligible in most cases except in the RO unit (which consumes only electricity). In table 8 it can be seen how wind contribution to cost formation increases, especially in components 2 and 9, although it is lower than the contribution of solar energy.

	Total unit exergy cost	Ideal	I1	I2	I3	I4	I5	I6	I7	I8	I9	I10	I11
P1. WT	**2.07**	1	1.07	0	0	0	0	0	0	0	0	0	0
P2. Elec.cont.	**5.32**	1	0.50	0.11	1.86	1.85	0	0	0	0	0	0	0
P3. PVT 1-2	**6.77**	1	0	0	5.77	0	0	0	0	0	0	0	0
P4. PVT 3-4	**6.72**	1	0	0	0	5.72	0	0	0	0	0	0	0
P5. ETC	**12.44**	1	0	0	0	0	11.4	0	0	0	0	0	0
P6. Solar loop	**15.10**	1	0.11	0.02	1.71	1.78	9.93	0.55	0	0	0	0	0
P7. HWT	**45.11**	1	0.32	0.72	5.11	5.31	29.7	1.65	1.99	0	0	0	0
P8. MD	**525.0**	1	4.17	0.93	60.6	62.9	342.0	19.0	22.9	11.4	0	0	0
P9. RO	**25.71**	1	2.41	0.54	9.01	8.92	0	0	0	0	3.83	0	0
P10. Mixer	**49.67**	1	1.13	0.25	7.73	7.89	26.8	1.49	1.80	0.25	1.31	0.01	0.01
P11. Tank	**56.95**	1	2.58	0.57	12.4	12.4	21.0	1.17	1.40	0.70	3.69	0	0.02

Table 7: Unit exergy cost decomposition according to irreversibilities for the complete year. Case of 800W wind turbine.

	Total unit exergy cost	Sun	Wind
P1. WT	**2.07**	0	2.07
P2. Elec.cont.	**5.32**	4.35	0.96
P3. PVT 1-2	**6.77**	6.77	0
P4. PVT 3-4	**6.72**	6.72	0
P5. ETC	**12.44**	12.44	0
P6. Solar loop	**15.10**	14.90	0.21
P7. HWT	**45.11**	44.49	0.62
P8. MD	**525.0**	516.9	8.06
P9. RO	**25.71**	21.05	4.66
P10. Mixer	**49.67**	47.50	2.17
P11. Tank	**56.95**	51.96	4.99

Table 8: Unit exergy cost decomposition according to external fuel for the complete year. Case of 800W wind turbine.

Tables 9 and 10 include the analysis of the unit exergy cost formation for the case where electricity consumed by solar loop is reduced. It can be seen how this plant modification causes a small reduction of the unit exergy cost of the product of MD and also (although negligible) in the products of solar loop, hot water tank, water tank and mixer.

	Total unit exergy cost	Ideal	I1	I2	I3	I4	I5	I6	I7	I8	I9	I10	I11
P1. WT	**2.07**	1	1.07	0	0	0	0	0	0	0	0	0	0
P2. Elec.cont.	**6.12**	1	0.32	0.11	2.36	2.33	0	0	0	0	0	0	0
P3. PVT 1-2	**6.77**	1	0	0	5.77	0	0	0	0	0	0	0	0
P4. PVT 3-4	**6.72**	1	0	0	0	5.72	0	0	0	0	0	0	0
P5. ETC	**12.44**	1	0	0	0	0	11.4	0	0	0	0	0	0
P6. Solar loop	**14.88**	1	0.05	0.02	1.66	1.73	9.93	0.49	0	0	0	0	0
P7. HWT	**44.45**	1	0.14	0.05	4.97	5.18	29.7	1.46	1.99	0	0	0	0
P8. MD	**518.0**	1	1.93	0.68	59.4	61.8	342.0	16.8	22.9	11.4	0	0	0
P9. RO	**29.58**	1	1.53	0.54	11.4	11.3	0	0	0	0	3.83	0	0
P10. Mixer	**50.40**	1	0.66	0.23	8.43	8.58	26.8	1.32	1.80	0.25	1.31	0.01	0.01
P11. Tank	**60.25**	1	1.59	0.56	14.6	14.7	21.0	1.03	1.40	0.70	3.69	0	0.02

Table 9: Unit exergy cost decomposition according to irreversibilities for the complete year. Case of improved solar loop.

	Total unit exergy cost	Sun	Wind
P1. WT	**2.07**	0	2.07
P2. Elec.cont.	**6.12**	5.51	0.61
P3. PVT 1-2	**6.77**	6.77	0
P4. PVT 3-4	**6.72**	6.72	0
P5. ETC	**12.44**	12.44	0
P6. Solar loop	**14.88**	14.79	0.09
P7. HWT	**44.45**	44.17	0.28
P8. MD	**517.98**	514.25	3.73
P9. RO	**29.58**	26.63	2.95
P10. Mixer	**50.40**	49.13	1.27
P11. Tank	**60.24**	57.18	3.07

Table 10: Unit exergy cost decomposition according to external fuel for the complete year. Case of improved solar loop.

Finally, Table 11 summarizes the main results of the four cases considered. Columns 2 and 3 indicate the fuel along a year according to its origin, solar or wind; it can be seen how the latter is much smaller than the former and how they vary when the size of ETC or wind turbine are varied. Colum 4 shows how electricity production during a year increases clearly when bigger wind turbine is used. Besides, it also increases around 100 MJ when electricity consumed by the solar (water-glycol) loop is reduced, whereas it has a negligible increment when the size of ETC is increased. Other plant

products (fresh water and sanitary hot water) ideally would be constant in the four cases, although some minor differences appear: fresh water exergy varies from 179.3 to 180.7 MJ per year, and hot water varies from 408.1 to 436.3 MJ per year. In the last columns, efficiency appears: conversion to fresh water, to sanitary hot water, to electricity and total (summation of the other three). It can be seen how the most relevant contribution to efficiency is electricity production. When ETC of 4.5 m^2 is introduced, fuel increases whereas product is constant, what leads to a reduction in efficiency. On the other hand, when the wind turbine size is increased, electricity production also increases, what leads to an increment of efficiency. Finally, solar loop improvement causes a small increment of electric and total efficiency. In fact, this latter change is relevant because it is the only of the proposed modifications that keeps constant the fuel supply. It should be highlighted that efficiency is not the only issue to be considered, mainly when solar and wind energy are used. For instance, when a bigger ECT is used, efficiency decreases but MD unit can be used during more hours.

	Fuel: solar (MJ)	Fuel: wind (MJ)	Product: electricity (MJ)	Efficiency (%)			
				Fresh water	SHW	Electricity	Total
Base case	50843	3339	3617	0.33	0.75	6.68	7.76
ECT 4.5	58854	3339	3629	0.29	0.70	5.84	6.83
WT 800W	50843	6678	5067	0.31	0.71	8.81	9.83
Improved solar loop	50843	3339	3713	0.33	0.72	6.85	7.93

Table 11: Comparison of main results: fuel and electricity produced during a year and efficiency.

4. Conclusion

Exergy and exergy cost analysis of the operation of a hybrid trigeneration system producing electricity, fresh water and hot water from PVT and ETC panels and a wind turbine has been presented. The study has been made by using simulation results obtained by a TRNSYS model of the system. Two time scales have been applied: detailed analysis with ten-minute evolution of the variables and aggregated analysis in monthly basis that summarizes in a single graph behavior during a year of the analyzed component. Results show that highest irreversibility appear in the collectors, what could be expected since they produce heat at low temperature; in this sense, PVT panels have much higher efficiency due to the joint production of hot water and electricity. A relevant source of irreversibility is the need of driving MD unit at suitable temperature, what in the present design is made through several steps (collectors, hot water tank and heat exchanger); a direct connection avoiding the tank would lead to lower irreversibility and higher productions.

Besides the base case, three additional examples have been analyzed: increment of ETC size (reduces efficiency but increases MD use), increment of wind turbine size (increases electricity production and, thus, global efficiency) and reduction of electricity consumed by the solar loop (what increases, although slightly, both electricity production and global efficiency).

The assessment of the system from the exergy and exergy cost point of view has allowed one to identify some weak points related to system efficiency, which is the first step for improving. It might seem that improving exergy efficiency is not relevant when resources such as wind and sun that are available for free are used. However, it should be noted that, although exergy entering the plant is for free, exergy flows

within the plant are not free because they have been produced by using pieces of equipment that require investment and maintenance. For instance, if a flow generated by a solar collector is not used properly, more solar collectors may be needed for covering the same heat or electricity demand. For this reason, looking for improvements in the use of resources throughout the plant is always interesting. Of course, this aim has to be considered by taking into account other issues such as investment, reliability, environmental impact or ability of the system to cover the required demands.

Finally, despite of potentials for improvement, it should be highlighted that in its present configuration the analyzed scheme is able to provide the three main products required in a house isolated from grids by applying a combination of existing technologies and with relatively good average global efficiency. The investment cost, although high, may become interesting when compared to the alternative supply by extending conventional networks up to isolated locations.

Acknowledgement

The authors wish to thank the financial support given by the Spanish Ministry of Economics and Competiveness in the framework of the “Retos de la Sociedad” R+D Program, under the TRHIBERDE R+D project (ENE2014-59947-R).

Nomenclature

A Area [m^2]

b Specific exergy [kJ/kg]

B Exergy flow [kJ]

$\dot{B}$ Exergy flow rate [kW]

c Specific heat [kJ/(kg·K)]

C	Concentration [g/L]
CSP	Concentrated solar power
DHC	District heating and cooling
E	Exergy flow in productive structure [kJ]
E^*	Exergy cost of streams [kJ]
ETC	Evacuated tube collector
F	Fuel [kJ]
$\dot{F}$	Fuel rate [kW]
$\boldsymbol{F}$	Vector of fuel (n × 1) [kJ]
F^*	Exergy cost of fuel [kJ]
FW	Fresh water
$\langle \boldsymbol{FP} \rangle$	Matrix of distribution coefficients (n × n) [-]
HWT	Hot water tank
HX	Heat exchanger
I	Irreversibility [kJ], solar radiation [kW/m_2]
$\dot{I}$	Irreversibility rate [kW]
$\boldsymbol{I}$	Vector containing the irreversibility of the components (n × 1) [kJ]
ICE	Internal combustion engine
k^*	Unit exergy cost [-]
$\dot{m}$	Mass flow rate [kg/s]
MD	Membrane distillation
MED	Multi-effect distillation
MW	Molecular weight [kg/kmol]
n	Number of components of the system [-]
n_f	Number of external resources [-]
ORC	Organic Rankine cycle
P	Product [kJ]
$\dot{P}$	Exergy rate [kW]
$\boldsymbol{P}$	Vector of product of the components (n × 1) [kJ]
P^*	Exergy cost of product [kJ]
$\boldsymbol{P}^*$	Vector of exergy cost of product (n × 1) [kJ]

PGMD Permeate gap membrane distillation

PV Photovoltaic

PVT Photovoltaic thermal

R Constant of gases [kJ/(kg·K)]

RC Recovery ratio

RDF Refuse derived fuel

RES Renewable energy sources

RO Reverse osmosis

SHW Sanitary hot water

SOC State of Charge

SOFC Solid oxide fuel cell

t Time [s]

T Temperature [K]

$\mathbf{U_D}$ Identity matrix ($n \times n$)

v velocity (m/s)

WT Wind turbine

y Distribution coefficient [-]

Greek symbols

β Number of particles [-]

η Efficiency [-]

ρ Density [kg/m^3]

Subscripts and superscripts

0 Environment, reference

av Average

C Component

ch Chemical

e Plant input

F Fuel

i Generic component

j Generic component

k Type of external resource

P Product

ph Physical

rad Radiation

s Surface

References

[1] Trujillo A, Domínguez I, Herrera T. Using TRNSYS® simulation to optimize the design of a solar water distillation system. Energy Procedia 2014;57:2441-2450.

[2] Liang R, Zhang J, Zhou C. Dynamic simulation of a novel solar heating system based on hybrid photovoltaic/thermal collectors (PVT). Procedia Engineering 2015;121:675-683.

[3] Astea N, Leonforte F, Pero C. Design, modeling and performance monitoring of a photovoltaic-thermal (PVT) water collector. Solar Energy 2015;112:85-99.

[4] Haurant P, Ménézo C, Gaillard L, and Dupeyrat P. A numerical model of a solar domestic hot water system integrating hybrid photovoltaic/thermal collectors. Energy Procedia 2015;78:1991-1997.

[5] Bakic V, Pezo M, Stevanovic Z, Zivkovic M, Grubor B. Dynamical simulation of PV/wind hybrid energy conversion system. Energy 2012;45:324-328.

[6] Huang Q, Shi Y, Wang Y, Lu L, Cui Y. Multi-turbine wind-solar hybrid system. Renewable Energy 2015;76:401-407.

[7] Raluy R, Schwantes R, Subiela V, Peñate B, Melián G, Betancort J. Operational experience of a solar membrane distillation demonstration plant in Pozo Izquierdo-Gran Canaria Island (Spain). Desalination 2012;290:1-13.

[8] Mohan G, Kumar U, Pokhrel M K, Martin A. A novel solar thermal polygeneration system for sustainable production of cooling, clean water and domestic hot water in United Arab Emirates: Dynamic simulation and economic evaluation. Applied Energy 2016;167:173-188.

[9] Palenzuela P, Alarcón-Padilla DC, Zaragoza G. Large-scale solar desalination by combination with CSP: Techno-economic analysis of different options for the Mediterranean Sea and the Arabian Gulf. Desalination 2015;366:130–138.

[10] Rym C, Dhaouadi H, Mhiri H, Bournot P. A TRNSYS Dynamic Simulation Model for Photovoltaic System Powering a Reverse Osmosis Desalination Unit with Solar Energy. International Journal of Chemical Reactor Engineering 2010;8:1-13.

[11] Manokar, A.M., Winston, D.P., Kabeel, A.E., Sathyamurthy, R. Sustainable fresh water and power production by integrating PV panel in inclined solar still. Journal of Cleaner Production 2018:172: 2711-2719.

[12] Rensonnet T, Uche J, Serra L. Simulation and thermoeconomic analysis of different configurations of gas turbine (GT)-based dual-purpose power and desalination plants (DPPDP) and hybrid plants (HP). Energy 2007;32:1012-1023.

[13] Jana, K., Ray, A., Majoumerd, M.M., Assadi, M., De, S. Polygeneration as a future sustainable energy solution – A comprehensive review. Applied Energy 2017:202: 88–111.

[14] Al-Sulaiman FA, Dincer I, Hamdullahpur F. Thermoeconomic optimization of three trigeneration systems using organic Rankine cycles: Part I – Formulations. Energy Conversion and Management 2013;69:199–208.

[15] Al-Sulaiman FA, Dincer I, Hamdullahpur F. Thermoeconomic optimization of three trigeneration systems using organic Rankine cycles: Part II – Applications. Energy Conversion and Management. 2013;69:209–216.

[16] Bicer Y, Dincer I. Analysis and performance evaluation of a renewable energy based multigeneration system. Energy 2016;94:623-632.

[17] Calise F, Dentice d'Accadia M, Piacentino A. A novel solar trigeneration system integrating PVT (photovoltaic/thermal collectors) and SW (seawater) desalination: Dynamic simulation and economic assessment. Energy 2014;67:129-148.

[18] Maraver D, Uche J, Royo J. Assessment of high temperature organic Rankine cycle engine for polygeneration with MED desalination: A preliminary approach. Energy Conversion and Management 2012;53 (1):108-117.

[19] Sahoo U, Kumar R, Pant PC, Chaudhury R. Scope and sustainability of hybrid solar–biomass power plant with cooling, desalination in polygeneration process in India. Renewable and Sustainable Energy Reviews 2015;51:304-316.

[20] Rubio C, Uche J, Martínez A, Bayod AA. Design optimization of a polygeneration plant fuelled by natural gas and renewable energy sources. Applied Energy 2011;88 (2):449-457

[21] Del Amo A, Martínez A, Bayod AA, Antoñanza J. An innovative urban energy system constituted by a photovoltaic/thermal hybrid solar installation: Design, simulation and monitoring. Applied Energy 2017;186:140-151

[22] Mohan G, Uday K, Manoj K, Martin A. Experimental investigation of a novel solar thermal polygeneration plant in United Arab Emirates. Renewable Energy 2016;91:361-373.

[23] Mohan G, Kumar U, Pokhrel M K, Martin A, 2016. A novel solar thermal polygeneration system for sustainable production of cooling, clean water and domestic hot water in United Arab Emirates: Dynamic simulation and economic evaluation. Applied Energy 167, 173-188.

[24] Szargut J. Exergy method: Technical and ecological applications. WIT Press, Southampton, 2005.

[25] Saloux E, Teyssedou A, Sorin M. Analysis of photovoltaic (PV) and photovoltaic/thermal (PV/T) systems using the exergy method. Energy and Buildings 2013;67:275-285.

[26] Sadri S, Ameri M, Khoshkhoo, R H. Multi-objective optimization of MED-TVC-RO hybrid desalination system based on the irreversibility concept. Desalination 2017:402:97-108.

[27] Banat F, Jwaied N. Exergy analysis of desalination by solar-powered membrane distillation units. Desalination 2008;230:27-40.

[28] Ortega-Delgado B, García-Rodríguez L, Alarcón-Padilla DC. Thermoeconomic comparison of integrating seawater desalination processes in a concentrating solar power plant of 5 MWe. Desalination 2016;392:102–117.

[29] Sharaf MA, Nafey AS, García-Rodríguez L. Exergy and thermo-economic analyses of a combined solar organic cycle with multi effect distillation (MED) desalination process. Desalination 2011;272 (1–3):135-147.

[30] Mokhtari H, Sepahv M, Fasihfar A. Thermoeconomic and exergy analysis in using hybrid systems (GT+MED+RO) for desalination of brackish water in Persian Gulf. Desalination 2016;399:1–15.

[31] Calise F, Dentice d'Accadia M, Libertini L, Quiriti E, Vicidomini M. A novel tool for thermoeconomic analysis and optimization of trigeneration systems: A case study for a hospital building in Italy. Energy 2017;126:64-87.

[32] Chitsaz A, Mehr AS, Mahmoudi, SMS. Exergoeconomic analysis of a trigeneration system driven by a solid oxide fuel cell. Energy Conversion and Management 2015;106:921-931.

[33] Kabalina N, Costa M, Yang W, Martin A, Santarelli M. Exergy analysis of a polygeneration-enabled district heating and cooling system based on gasification of refuse derived fuel. Journal of Cleaner Production 2017:141:760-773.

[34] Kallert A, Schmidt D, Bläse T. Exergy-based analysis of renewable multi-generation units for small scale low temperature district heating supply. Energy Procedia 2017:116:13-25.

[35] Al-Ali M, Dincer I. Energetic and exergetic studies of a multigenerational solar–geothermal system. Applied Thermal Engineering 2014;71 (1):16-23.

[36] Karellas S, Braimakis K. Energy–exergy analysis and economic investigation of a cogeneration and trigeneration ORC–VCC hybrid system utilizing biomass fuel and solar power. Energy Conversion and Management 2016;107:103-113.

[37] Khalid F, Dincer I, Rosen M A. Energy and exergy analyses of a solar-biomass integrated cycle for multigeneration. Solar Energy 2015:112:290-299.

[38] Calise F, Dentice d'Accadia M, Piacentino A. Exergetic and exergoeconomic analysis of a renewable polygeneration system and viability study for small isolated communities. Energy 2015;92:290-307.

[39] Calise F, Dentice d'Accadia M, Macaluso A, Piacentino A, Vanoli L. Exergetic and exergoeconomic analysis of a novel hybrid solar–geothermal polygeneration system producing energy and water. Energy Conversion and Management 2016;115:200–220.

[40] Behnam P, Arefi A, Shafii M B. Exergetic and thermoeconomic analysis of a trigeneration system producing electricity, hot water, and fresh water driven by low-temperature geothermal sources. Energy Conversion and Management 2018:157:266-276.

[41] Tribus M, Evans RB. A contribution to the theory of thermoeconomics. Technical report, Report no. 62-63; Department of Engineering, UCLA: Los Angeles, CA, USA, 1962.

[42] Valero A, Lozano M, Muñoz M. A general theory of exergy saving. Part I: On the exergetic cost. In: Computer Aided Engineering and Energy Systems, Vol. 3: Second Law Analysis and Modeling; Gaggioli R. Ed.; ASME: New York, NY, USA, 1986; vol. 2-3: 1-8.

[43] Torres C. Symbolic thermoeconomic analysis of energy systems. In: Frangopoulos CA, Ed. Exergy, energy system analysis and optimization, from Encyclopedia of life support systems (EOLSS). Oxford: EOLSS Publishers; 2006.

[44] Torres C, Valero A, Rangel V, Zaleta A. On the cost formation process of the residues. Energy 2008; 33: 144-152.

[45] Usón S, Valero A, Agudelo A. Thermoeconomics and industrial symbiosis. Effect of by-product integration in cost assessment. Energy 2012;45:43-51.

[46] Wang J, Mao T. Cost allocation and sensitivity analysis of multi-products from biomass gasification combined cooling heating and power system based on the exergoeconomic methodology. Energy Conversion and Management 2015;105:230–239.

[47] Beretta GP, Iora P, Ghoniem AF. Allocating resources and products in multi-hybrid multi-cogeneration: What fractions of heat and power are renewable in hybrid fossil-solar CHP?. Energy 2014;78:587–603.

[48] Wang Y, Lior N. Fuel allocation in a combined steam-injected gas turbine and thermal seawater desalination system. Desalination 2007;214 (1): 306–326.

[49] Piacentino A. Application of advanced thermodynamics, thermoeconomics and exergy costing to a Multiple Effect Distillation plant: In-depth analysis of cost formation process. Desalination 2015;371:88–103.

[50] Uche J, Serra L, Valero A. Exergy Costs and Inefficiency Diagnosis of a Dual-Purpose Power and Desalination Plant. Journal of Energy Resources and Technology 2005;128(3):186-193

[51] Leiva-Illanes R, Escobar Cardemil JM, Alarcón-Padilla DC. Thermoeconomic assessment of a solar polygeneration plant for electricity, water, cooling and heating in high direct normal irradiation conditions. Energy Conversion and Management 2017;151:538–552.

[52] Acevedo L, Uche J, Del Almo A, Círez F, Usón S, Martínez A, Guedea I. Dynamic Simulation of a Trigeneration Scheme for Domestic Purposes Based on Hybrid Techniques. Energies 2016;9:1013.

[53] Meteonorm database. www.meteonorm.com

[54] González F, Rueda T, Les S. Microcomponentes y factores explicativos del consumo doméstico de agua en la Comunidad de Madrid (in Spanish). Cuadernos de I+D+I. Canal de Isabel II. Madrid, Spain. 2008.

[55] Villagarcia C. Atlas de la demanda eléctrica. Proyecto INDEL (in Spanish). Red electrica de España, Madrid, 1998.

[56] Boletín Oficial del Estado (2017). Resolución de 28 de diciembre de 2016, donde se aprueba para el año 2017 el perfil de consume y método de cálculo a

efectos de liquidación de energía (in Spanish). Ministerio de Energía, Turismo y Agenda Digital, España.

[57] Petela R. Exergy of heat radiation. Journal of Heat Transfer 1964;86;187-192.

[58] Magdi Ragheb and Adam M. Ragheb (2011). Wind Turbines Theory - The Betz Equation and Optimal Rotor Tip Speed Ratio, Fundamental and Advanced Topics in Wind Power, Dr. Rupp Carriveau (Ed.), ISBN: 978-953-307-508-2, InTech, Available from: http://www.intechopen.com/books/fundamental-and-advanced-topicsin-wind-power/wind-turbines-theory-the-betz-equation-and-optimal-rotor-tip-speed-ratio.

[59] Liu J, Yuan J, Xie L, Yi Z. Exergy analysis of dual-stage nanofiltration seawater desalination. Energy 2013;62:248-254.

[60] Carrasquer B, Martínez A, Uche J. Exergy costs analysis of water desalination and purification techniques by transfer functions. Energy Conversion and Management 2016;126:51-59